AEROHEAD AERONAUTICS

AA SB-01©

Response to 2008/2009 AIAA Foundation Undergraduate Team Aircraft Design Competition
Presented by Virginia Polytechnic Institute and State University

©

TEAM AEROHEAD AERONAUTICS©

From left to right: Matthew Freeze, Brian Leslie, Robert Yager, Robert Lewandowski, John Blizard, and Daniel Aiken

Daniel Aiken
Cost Evaluation
Propulsion
AIAA member #: 307195

John Blizard
Team Lead
Stability and Control
Noise Analysis
AIAA member # 307219

Matthew Freeze
Mission Systems
Flight Performance
Materials
AIAA member #: 307177

Brian Leslie
Aerodynamics
Structures
AIAA member #: 307181

Robert Lewandowski
Configuration Designer
AIAA member #: 307180

Robert Yager
Weight Sizing
Propulsion
AIAA member #: 269269

Dr. William Mason
Project Advisor
AIAA member #: 11141

Dr. Mayuresh Patil
AIAA Advisor
AIAA member #: 144995

Executive Summary

Aerohead Aeronautics received the request for proposal (RFP) from the American Institute of Aeronautics and Astronautics (AIAA) on September 30, 2008. It calls for the development of a new commercial airliner capable of seating 150 passengers and entering service in 2018. This vehicle is currently in high demand throughout the industry due to the fatigue of existing aircraft that do not meet growing economic and environmental concerns. The RFP requires a reduction of both cost and emissions for the future of air travel and Aerohead Aeronautics is pleased to present a satisfying response. This regional transportation aircraft will have the range capability to traverse the United States (2800 nm) while reducing noise and environmental emissions and maintaining low fuel consumption. For the aircraft to meet design criteria, it must meet noise regulations set forth by ICAO (International Civil Aviation Organization) Chapter 4 minus 20dB cumulative. The RFP's goal is to achieve a long range cruising speed of 0.8 Mach. It shall have a balanced field length (BFL) of no more than 7000 feet and a minimum approach speed of 135 knots. It is also required to have an initial cruising altitude of 35,000 feet and a maximum operating ceiling of 43,000 feet. Per seat operational costs shall be 10% lower than existing aircraft and the designed aircraft meet all Federal Aviation Regulations (FAR). The Aerohead concept consists of a strut-braced wing, which has been used on small and military aircraft but has not been applied to the commercial airliner industry. The weight and aerodynamic characteristics of a strut-wing model were compared to those of existing and proposed wing configurations, but the strut-braced design demonstrated some superiorities. Aerohead Aeronautics will employ advanced technologies throughout the design to ensure that the passenger transport will not only meet the demands of the AIAA RFP, but also those of the everyday passenger. Aerohead Aeronautics presents the SB-01.

	Units	Wing	Horizontal Tail	Vertical Tail
Area	ft^2			
Reference	ft^2	1699	386.3	250.2
Whetted	ft^2	4985.7	780.2	505.4
Span	ft	136.37	40.68	18.48
Aspect Ratio	–	11	4.3	1.36
Taper Ratio	–	.25	.40	.64
Thickness-to-Chord Ratio	–	.09	.05	.05
Chord Length	ft	–	–	–
Root	ft	19.83	11.25	10.33
Tip	ft	4.96	4.50	6.58
MAC	ft	12.42	7.38	8.46
1/4 Chord Sweep	deg	18	17	23
Anhedral	deg	3	–	–

AEROHEAD AERONAUTICS

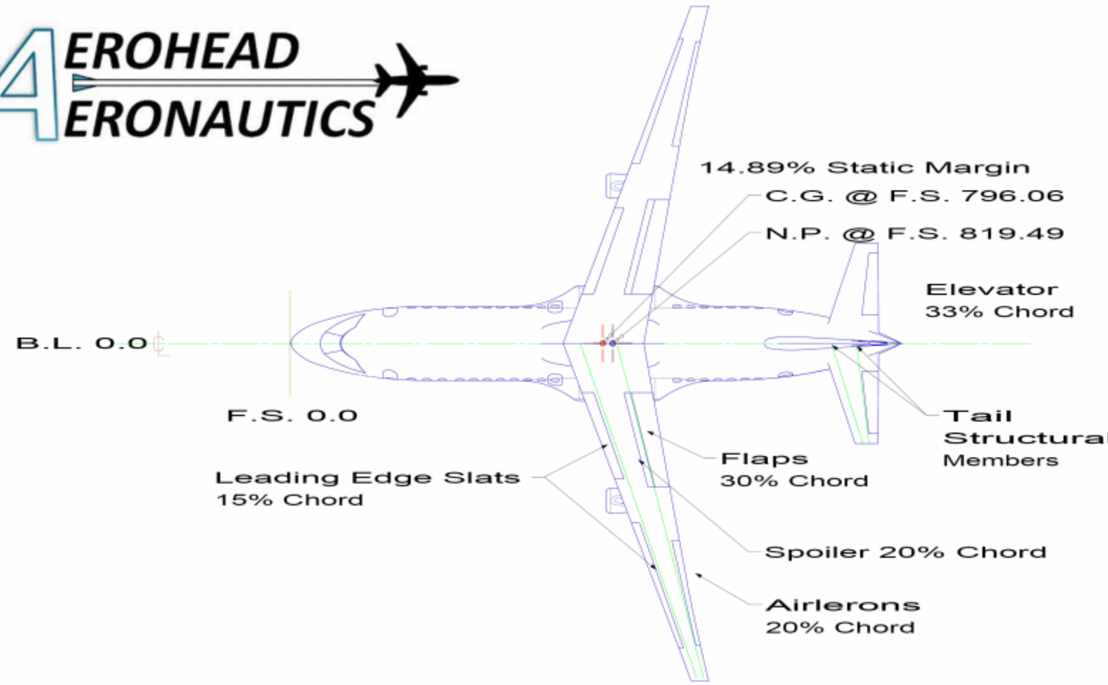

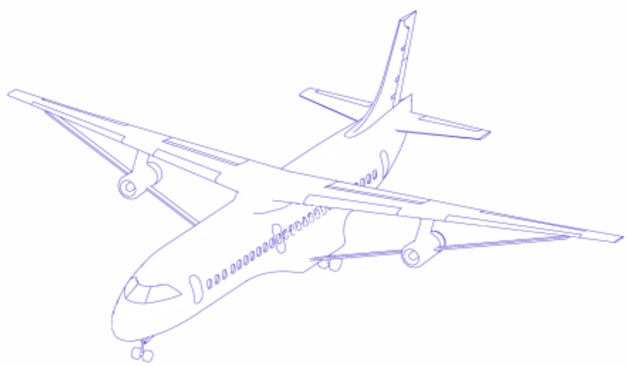

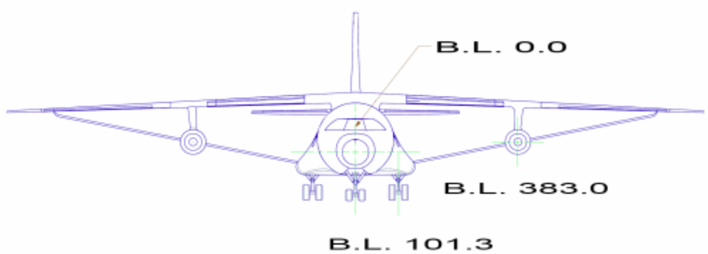

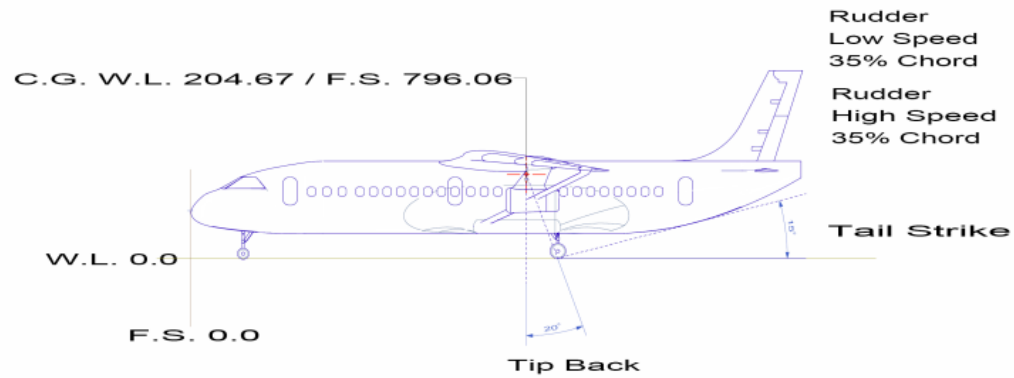

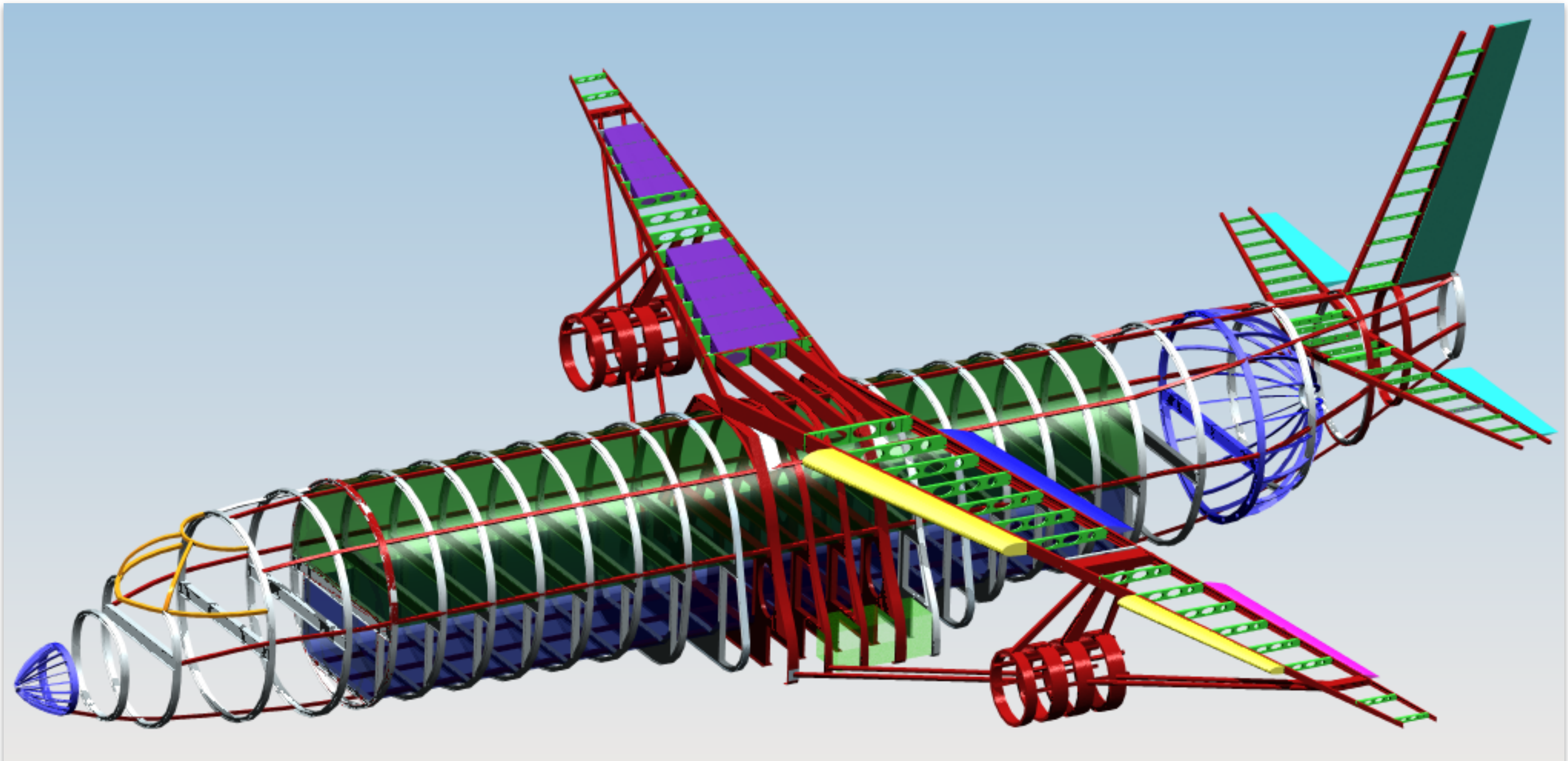

Main Load Bearing Members	Red		**Passenger Seating Area**	Transparent Green
Leading Edge Slats	Yellow		**Cargo Hold**	Transparent Blue
Trailing edge Flaps	Blue		**Landing Gear Pod**	Transparent Green
Ailerons	Magenta		**Rudder**	Teal
Pressure Bulkheads	Blue		**Elevator**	Cyan
Fuel Tanks	Purple		**Strut**	Red
Flight Deck	Orange			

Table of Contents

Index of Figures

Index of Tables

Abbreviations

AIAA – *American Institute of Aeronautics and Astronautics*
ANOPP – Aircraft Noise Prediction Program
APS – Air Purification System
APU – Auxiliary Power Unit
BFL – Balanced Field Length
BWB – Blended Wing Body
CFRP – Carbon Fiber Reinforced Plastic
CFRP – Carbon Reinforced Plastic
CG – Center of Gravity
EBHA – Electro-backup-hydrostatic Actuator
EHA – Electro-hydrostatic Actuator
FAA – Federal Aviation Administration
FAR – Federal Aviation Regulations
FML –Fiber Metal Laminate
GFP – Graphical Flight Planning
GLARE – Glass Reinforced Fiber Metal Laminate
ICAO – International Civil Aviation Organization
INAV – Integrated Navigation
LCD – Liquid Crystal Display
LED – Light-emitting Diode
LRC – Long Range Cruise
MAC – Mean Aerodynamic Chord
MFRD – Multifunction Radar Display
MTOW – Maximum Take-off Weight (lbs)
N.P. – Neutral Point
NASA – National *Aeronautics and Space Administration*
PCU – Power Control Unit
RFP – Request For Proposal
S.M. – Static Margin
THSA – Trimmable Horizontal Stabilizer Actuator
TOGW – Take Off Gross Weight
TRA – Terrain Radio Altitude
VIA – Versatile Integrated Avionics
LCC – Life Cycle Cost
RDTE – Research Development Testing Evaluation
ASM – Available Seat Mile
DOC – Direct Operating Cost
IOC – Indirect Operating Cost
AEP – Aircraft Estimated Price

Nomenclature

AR – Aspect Ratio
b – Wing Span
c – Chord (ft)
C_{acq} – Acquisition Cost
C_{D0} – Coefficient of Profile Drag
C_{Di} – Coefficient of Induced Drag
C_D – Coefficient of Drag
C_{Dtrim} – Coefficient of Trim Drag
C_{Dw} – Coefficient of Wave Drag
C_{Lmax} – Maximum Coefficient of Lift
C_{Lp} – Lift Coefficient due to Pitch
C_{Lr} – Lift Coefficient due to Rudder
$C_{L\alpha}$ – Lift Coefficient due to Angle of Attack
$C_{L\beta}$ – Lift Coefficient due to Sideslip
$C_{L\delta r}$ – Lift Coefficient with Rudder Deflection
C_{Mq} – Moment Coefficient due to Pitch
$C_{M\alpha}$ – Moment Coefficient due to Angle of Attack
C_{Navail} – Yawing Moment Available
C_{Np} – Yawing Coefficient due to Pitch
C_{Nr} – Yawing Coefficient due to rudder
$C_{Nrequired}$ – Yawing Moment Required
$C_{N\beta}$ – Yawing Coefficient due to Sideslip
$C_{N\delta r}$ – Yawing Coefficient due to Rudder Deflection
C_{opsdir} – Indirect Operating Costs

e – Oswald's efficiency factor
g – Gravity (ft/s^2)
k_A – Airfoil Technology Factor
L/D – Lift to Drag Ratio
l_{to} – Take-off Field Length (ft)
M – Mach Number
M_{crit} – Critical Mach Number
M_{DD} – Drag Divergence Mach Number
N_{yr} – Number of Years Aircraft is Operated
R_{bl} – Total Annual Block Miles Flown (nm)
S – Wing Area (in^2)
t/c – Thickness to Chord Ratio
T/W – Thrust to Weight
T_c – Thrust at Cruise (lbs)
T_o – Thrust at Take-off (lbs)
V_A – Approach Velocity (knots)
W – Weight (lbs)
W/S – Wing Loading
W_{empty} – Empty Weight of Aircraft (lbs)
W_{fixed} – Fixed Weight (lbs)
W_{fuel} – Weight of Fuel (lbs)
β – Sideslip angle
δa – Aileron Deflection
δr – Rudder Deflection
Λ – Wing Sweep
ρ_{sl} – Density at Sea Level (slug/ft^3)
σ – Density Ratio
φ – Flight path angle

I. Introduction

The first American commercial transport consisted of one passenger being transported from St. Petersburg to Tampa, Florida in the winter of 1914. The actual flight lasted no longer than 23 minutes from start to finish and did not exceed an altitude of 15 feet. Since this flight, the demands of air travel have changed drastically to meet the needs of the modern day population. These demands include but are not limited to increases in range, speed, fuel efficiency, passenger comfort as well as decreases in noise and engine emissions.

Considering the current status of the economy and the fluctuating prices of oil, the transportation industry is in dire need of a fuel efficient solution that is comparable or cheaper in price to current aircraft. As numerous companies compete to fulfill this demand, several designs are being considered and analyzed to determine the direction and the future of the airline industry.

1.1 RFP Analysis

The American Institute of Aeronautics and Astronautics RFP calls for a new transcontinental commercial transport system capable of comfortably accommodating 150 passengers in a dual class seating arrangement. The current aircraft design must show significant improvements in fuel burn efficiency and passenger comfort while reducing community noise and CO_2 emissions. To enter the competitive market for commercial transports, the design must be comparable or more desirable to current aircraft in terms of price, production, and performance utilizing existing infrastructure.

Specifically the RFP states that the aircraft must accommodate 12 first class passengers with 36” pitch seats and 138 passengers with 32” pitch seats. An additional design may be

proposed to accommodate a single class greater than 150 passengers with 30” pitch seats. These pitch requirements are typically standard for passenger aircraft regardless of the total capacity.

The vehicle must support the weight of the single class arrangement assuming an average passenger weight of 185 pounds and an average cargo density of 8 pounds per cubic foot. The maximum weight of the passenger payload is estimated as a full dual class passenger capacity assuming an average passenger weight of 225 pounds. The minimum requirement for cargo capacity is 7.5 cubic feet per passenger.

Range requirements of the aircraft state that 50% of all missions will be 500 nautical miles, 40% will be 1000 nautical miles, and 10% will be 2000 nautical miles. The maximum range of the vehicle is 2800 nautical miles including typical mission reserves and a full dual class passenger load at the higher weight average. It is required that the vehicle traverses these ranges at a LRC speed of Mach 0.78, yet it is desired that the aircraft obtain an LRC Mach of 0.80. The initial cruise altitude must be greater than 35,000 feet at a temperature 15ºC greater than the standard temperature at that altitude. The RFP requires the maximum operating altitude of the vehicle to be 43,000 feet. It is also required that the design be capable of landing at a speed less than 135 knots at the maximum landing weight.

Specifications state that the aircraft must takeoff in no longer than 7000 feet at sea level conditions and 86º F. The noise produced by the aircraft design must be cumulatively reduced 20 decibels from the ICAO Chapter 4 standards, which are simply 10 decibels lower than the Chapter 3 standards. The 20 decibel requirement must consist of the sum of the reductions from flyover, sideline, and approach noise with at least a one decibel reduction from each. A large portion of the noise signatures may be reduced from the engine selection alone. It is required

that the fuel burn block fuel per seat on each 500 nautical mile mission must be less than 41 pounds, yet it is desired that this number be reduced to 38 pounds per seat.

Overall, the designed aircraft must be certifiable to the appropriate FAA regulations for entry into service by 2018. The vehicle must reduce the total operational cost by at least 8% per seat, yet 10% is the desired reduction from the comparably sized commercial transports currently operating within the United States. A variety of engines may be selected yet the total acquisition cost of the airplane must be appropriate with respect to current 150 seat category transports. Considering the specifications mentioned above, the mission profile for the 2008-2009 AIAA Competition looks as shown in Figure 1.1.

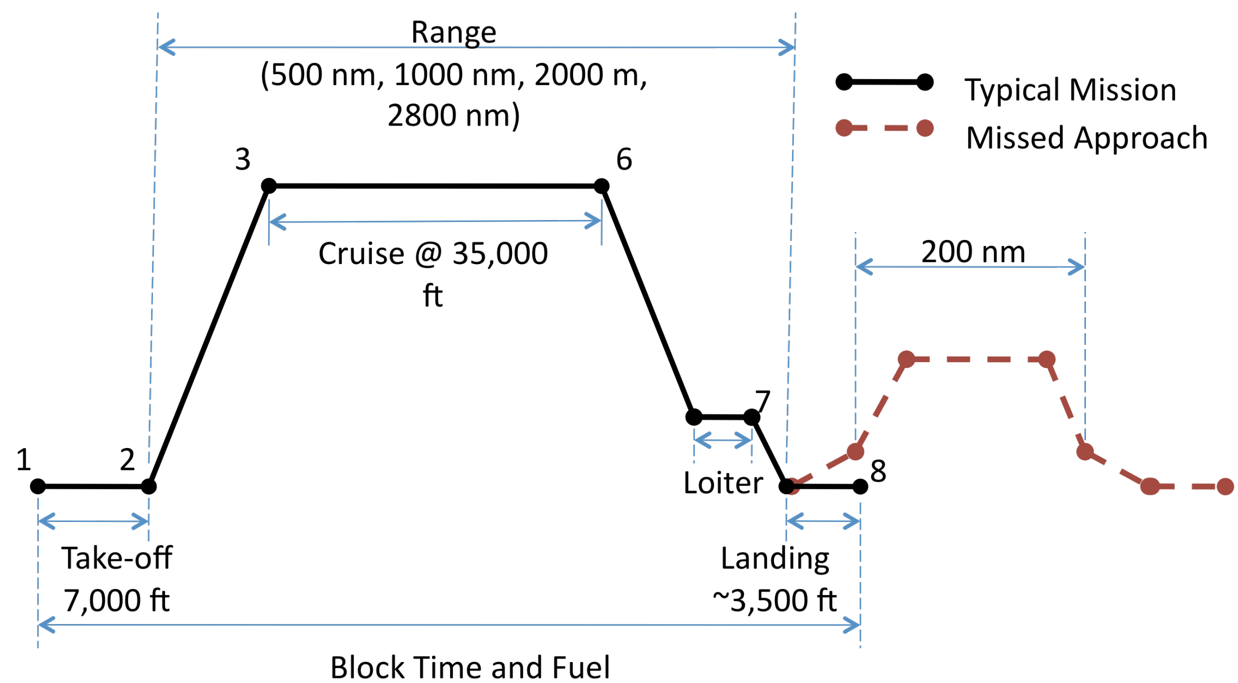

Figure 1.1 Mission profiles for the 2008-2009 AIAA Competition

2. Design Evolution

The design process began with each member of the group forming their own ideas and sketches of what kind of aircraft would best meet the RFP requirements. The six members each submitted their results for group evaluation. Of the six proposed designs concepts, only three were chosen. These three initial designs can be found on the next few pages, consisting of a cantilever wing, a strut-braced wing, and a blended wing body configuration. Analysis of these three designs found that each was capable of fulfilling the RFP.

2.1 Cantilever Design Concept

This concept is based on what has dominated the commercial aviation industry for decades. A cantilever design is the most commonly used passenger aircraft today. It consists of a cantilever wing with engines mounted below the wing to reduce wing box structure. The control surfaces are similar to the Boeing 737 series family in dimensions. Most of the advancements in efficiency come from the specific engines that are selected to power the aircraft and the materials used to construct the aircraft.

Table 2.1 Characteristics of Current Cantilever Wing Configuration Aircraft

Name	**Airbus A320-200**	**Boeing 737-400**	**Airbus A321**	**Bombardier C130**	**Tupolev 204-120**
Seat Capacity	150 (2-class)	159 (1-class)	185 (2-class)	130	160 (1-class)
Length (ft)	123	120	146	127.17	151.38
Wingspan (ft)	111.83	119.5	111.83	116	134.13
Fuselage Width (ft)	13	12.33	13	11.33	12.46
Empty weight (lb)	93,060	73,040	108,465	N/A	129630
MTOW (lb)	169,000	149,710	182,985	120,600	227,075
Cruising speed (Mach)	0.78	0.74	0.78	0.78	0.68
Max. speed (Mach)	0.82	0.82	0.82	0.82	N/A
Take off run @ MTOW (ft)	6,857	8,483	7,285	5,200	5,775
Range @ Max Capacity (nm)	3,000	2,165	2,138	1,800	2,321
Maximum Fuel Capacity (ft^3)	1048	818	837	N/A	N/A
Service Ceiling (ft)	39,000	37,000	39,800	41,000	39,700
Engines	CFM56-5	CFM56-3B-2	IAEV2530-A5	Turbofan	RB211 -535B75
Number of Engines	2	2	2	2	2
Thrust Rating (lbf)	26,250	22,000	29,900	20,500	42,580

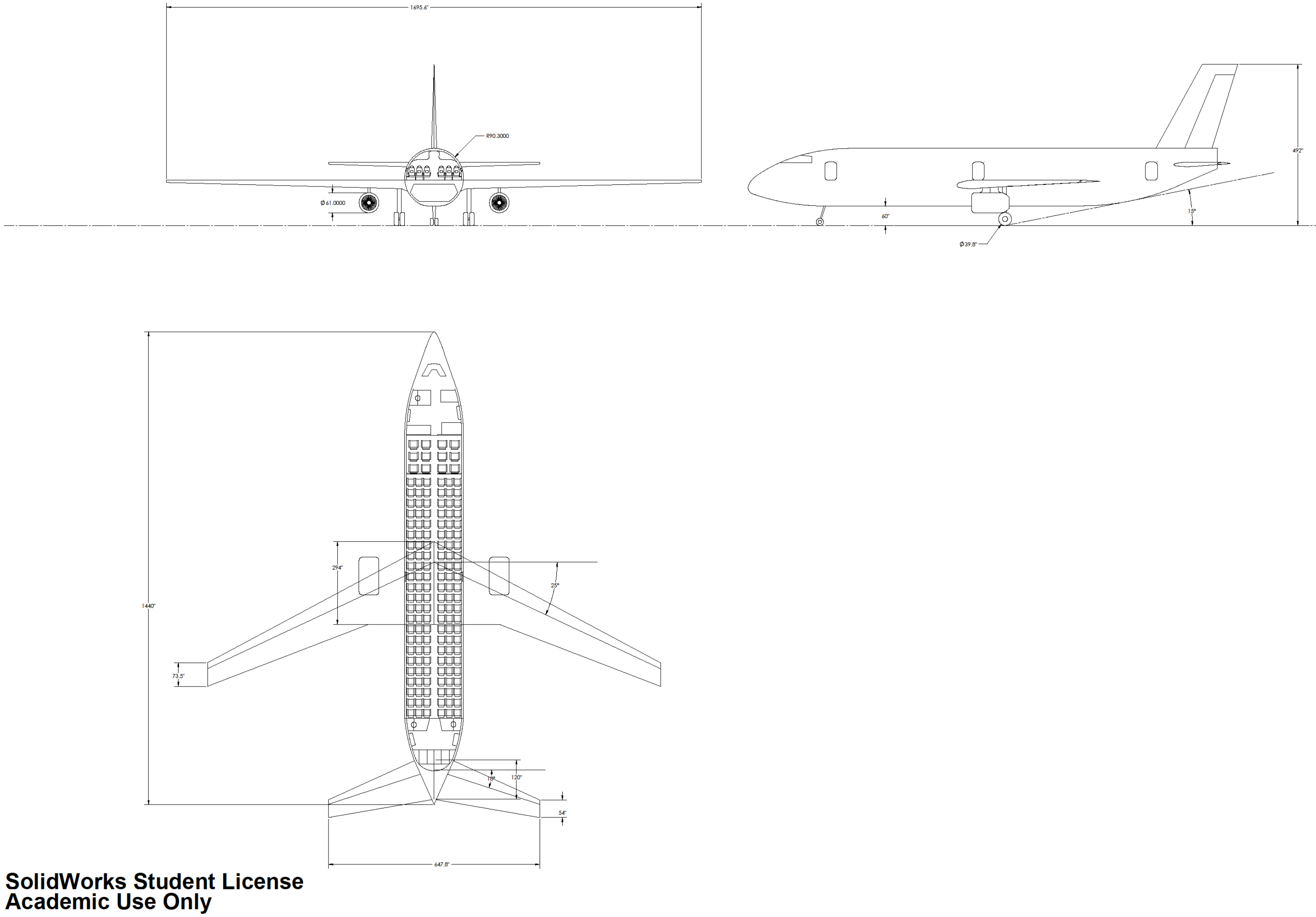

Figure 2.1 Aerohead Cantilever Concept

2.2 Blended Wing Body Concept

This concept uses a wing that blends into the fuselage, with the whole body acting as a lifting surface. Advantages of this aircraft are the improvements in fuel economy, lift at low speeds, and noise. Fuel economy is improved by reducing the weight and the wetted area of the aircraft. By decreasing the wing loading on the surfaces of the aircraft, there is a potential to lessen the amount of structural material required. This configuration also has a potential to diminish noise due to the smooth transition from the fuselage to the wing and the absence of high lift devices, such as flaps. The engines can be mounted on top of the aircraft which projects the engine noise upward, directing sound waves away from the ground. One of the potential draw backs of the BWB is its structural complexity resulting in cost increase. This concept's fuselage is also not an ideal pressure holding vessel, unlike the conventional cylinder shape. The BWB tends to receive more gains from its unconventional ideas as its size increases; however, it has not been proven in the industry yet. For a 150 passenger aircraft, one of the smallest of commercial airlines, the potential of the BWB is incredibly limited.

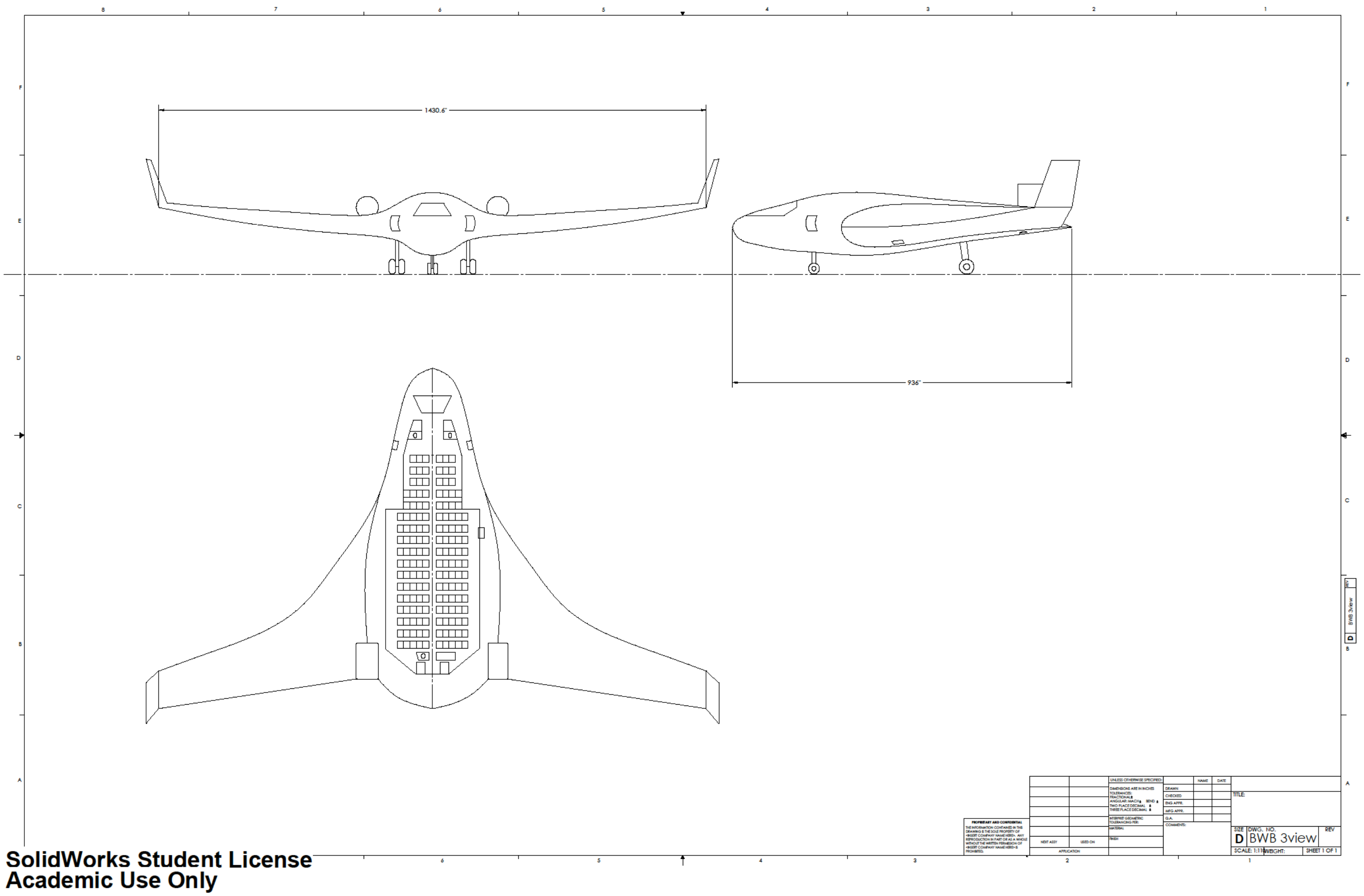

Figure 2.2 Aerohead BWB Concept

2.3 Strut-Braced Wing Concept

The main focus of the strut-braced wing concept is an added strut on the underside of the wing that acts as a tension bearing member. This strut reduces the need for structural reinforcement within the wing box which will decrease the overall weight of the aircraft significantly. With less strength required in the wing box a thinner wing can be used and the span can be increased. Small thickness to chord ratios permit this concept the ability to reduce the wing sweep required at Mach 0.78 to 0.80 in comparison with the conventional cantilever concept and blended wing body. A smaller thickness equates to increase of the drag divergence Mach number and a decrease in overall drag on the aircraft wing. Larger aspect ratios, resulting in high lift to drag values, make this concept an attractive choice for further investigation. The strut-braced wing concept does, however, have its drawbacks. Interference drag produced by the strut-wing joint requires detailed analysis along with the engine placement and strut-fuselage integration. Analysis of these obstacles was required to progress further in the design process and to provide an accurate comparison between configurations.

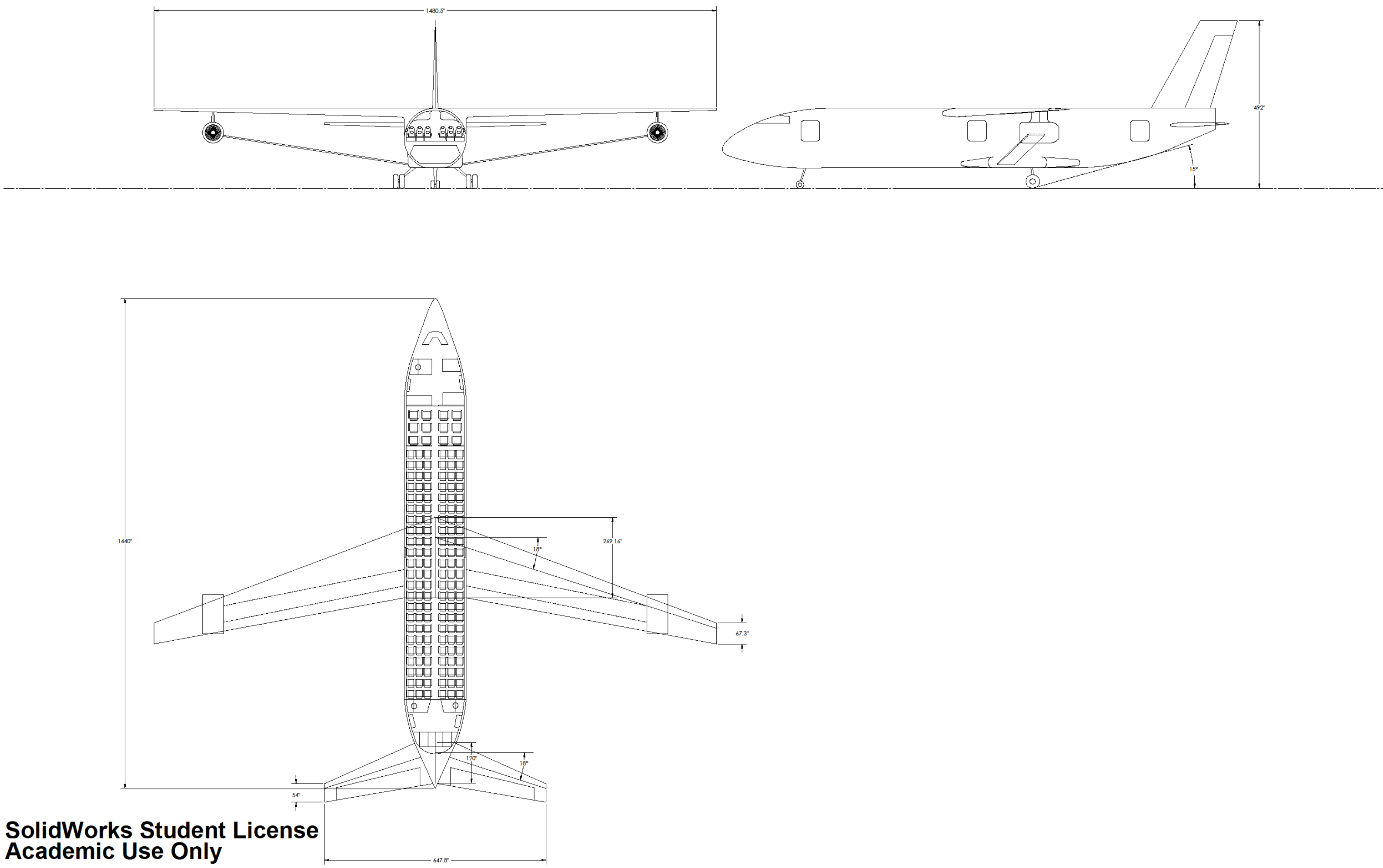

Figure 2.3 Aerohead Strut-Braced Concept

2.4 Initial Design Sizing

To find the proper size and dimensions of the aircraft for this design project, the Boeing 737-700 and the Airbus A320-200 were chosen because of their similar characteristics to the RFP requirements. From historcial data of these airplanes and our three preliminary designs, Thrust-to-Weight and Wing Loading plots were made to estimate the intial size of each design. The following equations[2] are used to plot the line for cruise comparing the T/W and W/S:

[illegible] $=$ [illegible] $40,000$ [illegible] $+1$ [illegible] (2.1)

[illegible] $=12$ [illegible] (2.2)

[illegible] $40,000=12$ [illegible] $40,000$ [illegible] 2 (2.3)

In these equations, C_{D0} and AR are shown in Table 5.1 for each airplane concept. The efficiency factor is 0.83. T_c and T_o have the values of 5480 lbs and 24,000 lbs. These thrust values are based on the CFM56-7B24[3]. The density, ρ, at 40,000 feet is 0.0005857 slug per cubic foot. To find the range of take-off constraint lines, the following equations are used:

[illegible] $=$ [illegible] (2.4)

[illegible] $=1$ [illegible] (2.5)

In the previous equations, σ has a value of one, assuming sea level. The Cl_{max} for take-off has a range from 0.5 to 1.0. The [illegible] has a length of 7000 feet. The density at sea level, [illegible] has a value of 0.002378 slug per cubic foot and the acceleration of gravity, g, is 32.2 feet per second. The final lines represent the comparison of T/W to W/S for the landing run:

[illegible] $=$ [illegible] 17.152 [illegible] (2.6)

The V_A has a value of 135 knots and the Cl_{max} for landing ranges from 1.5 to 2.5.

The design point on the thrust-to-weight versus wing loading plot needs to be chosen very carefully. It is desired to have a high wing loading for cruise, while having a lower wing loading for a slower approach to land. For the strut-braced wing design, the approximate values that were chosen are *T/W*=0.26 and *W/S*=99. The chosen location is shown by the black dot in Figure 2.4.

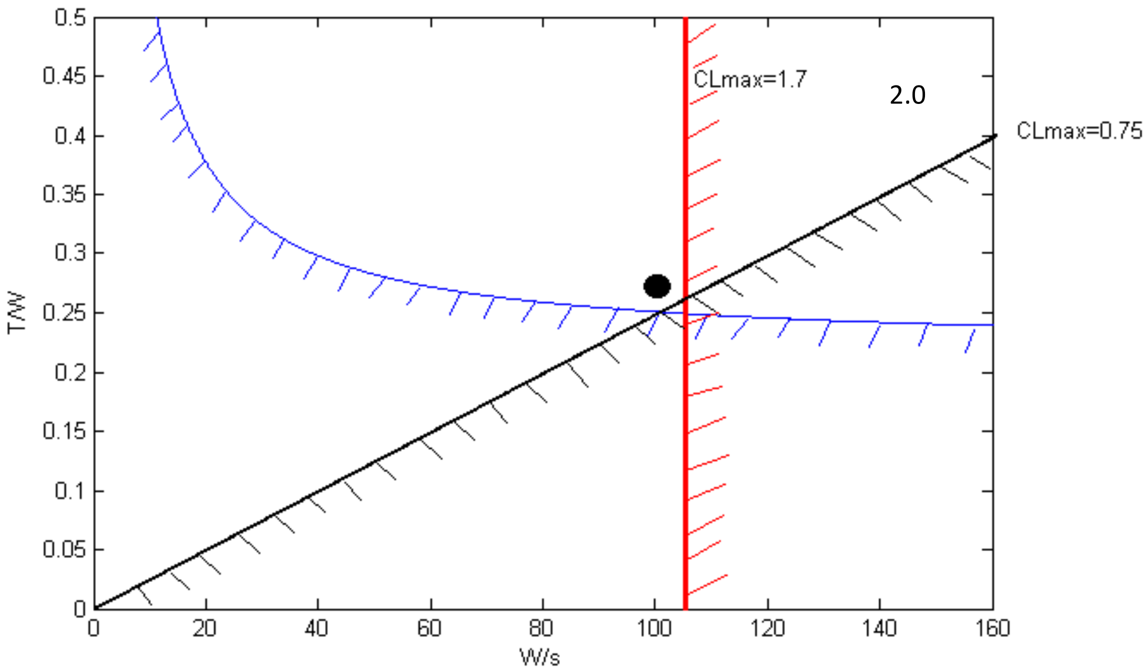

Figure 2.4 Plot of the T/W vs. W/S for Strut-braced Wing Design

2.5 Initial Design Weights

Intial weight estimates are compared for all three designs: Strut-braced Wing, Cantilever Wing, and Blended Wing Body, to each other and against the Boeing 737-700 and the Airbus A320-200. These estimates are made using the *Nicolai's* aircraft sizing algorithm[13]. The program derives estimates of the fuel weight, the empty weight, and the TOGW. Table 2.2 shows the list of parameters that change between each design when placed in the program.

Table 2.2 Parameters of the Nicolai Aircraft Sizing Program

	Strut-Braced	Cantilever	BWB	737-700[14]	A320-200[15]
Passengers	150	150	150	149	148
W_{fixed}	36,750	36,750	36,750	36,505	36,260

Cruise Mach #	0.8	0.8	0.8	0.785	0.78
Aspect Ratio	11	9.5	8	9.45	9.48
C_{D0} subsonic	0.018	0.016	0.02	0.016	0.016
dynamic pressure (psf)	223.3	223.3	223.3	223.3	223.3
speed of sound (ft/sec)	971	971	971	971	971
Subsonic SFC	0.37	0.37	0.37	0.37	0.37

From these parameters, the program was run for each design at regular and high capacity seating for the travel distances of 500 nm, 1000 nm, 2000 nm, and 2800 nm. The results of the program for each design with regular capacity seating for a 2800 nm trip is shown in Table 2.3.

Table 2.3 Results from *Nicolai* Sizing Program for 2800 nautical miles and Regular Capacity

Parameters	Strut-Braced	Cantilever	BWB	737-700	A320-200
W_{fuel} (lbs)	35,822	36,472	47,573	37,223	37,210
W_{empty} (lbs)	50,669	51,083	58,113	51,406	51,241
TOGW (lbs)	123,241	124,304	142,435	125,133	124,711

When examining these results, the strut-braced degin is calculated to have a 3.91%, 1.45% and 1.51% decrease in fuel weight, empty weight, and TOGW respectively versus the 737-700. It also has a 3.87%, 1.13% and 1.19% decrease in fuel weight, empty weight, and TOGW respectively versus the A320-200.

For the cantilever wing design, it has a 2.06%, 0.63% and 0.67% decrease in fuel weight, empty weight, and TOGW, respectively, versus the 737-700. It also has a 2.02%, 0.31% and 0.33% decrease in fuel weight, empty weight, and TOGW, respectively, versus the A320-200. When examining the blended wing body design results, it has a 21.76%, 11.54% and 12.15% increase in fuel weight, empty weight, and TOGW, respectively, versus the 737-700. It also has a 21.78%, 11.82% and 12.44% increase in fuel weight, empty weight, and TOGW, respectively, versus the A320-200. From these percentages, the strut-braced wing is shown to have the

highest decrease in weight, while the blended wing body has the highest. A downfall of the blended wing body in terms of weight is that it is usually designed to hold about 250 or more passengers, but in this case there are only 150 passengers. This is the reason why the blended wing body has such a high weight compared to the other aircraft designs.

The results from the *Nicolai* sizing program for the strut-braced wing design is compared with the Boeing 737-700 and Airbus A320-200 in Tables 2.4 to 2.6 for 500 nm, 1000 nm and 2000 nm.

Table 2.4 Results from *Nicolai* Sizing Program for 500 nautical miles and Regular Capacity

Weight	**Strut-Braced**	**737-700**	**A320-200**
W_{fuel} (lbs)	9,951	10046.23	10001.13
W_{empty} (lbs)	33,887	33788.11	33596.05
TOGW (lbs)	80,589	80339.19	79857.02

Table 2.5 Results from *Nicolai* Sizing Program for 1000 nautical miles and Regular Capacity

Weight	**Strut-Braced**	**737-700**	**A320-200**
W_{fuel} (lbs)	14277.34	14535.582	14487.813
W_{empty} (lbs)	36739.156	36747.841	36555.516
TOGW (lbs)	87766.321	87788.23	87303.135

Table 2.6 Results from *Nicolai* Sizing Program for 2000 nautical miles and regular capacity

Weight	Strut-Braced	737-700	A320-200
W_{fuel} (lbs)	24858.24	25610.27	25569.68
W_{empty} (lbs)	43631.68	43959.32	43774.80
TOGW (lbs)	105239.75	106074.43	105604.31

From examining these values, the percentage of weight that is decreased between the strut-braced design and the 737-700 and the A320-200 for each distance can be seen in Table 2.7. In this table, the positive values show the percent decrease in weight, and the negative values show a percent increase in weight.

Table 2.7 Weight Comparison for Strut-braced and Existing Aircraft for Mission Ranges

	500 nm		1000 nm		2000 nm	
% Savings, Strut-braced vs.	737-700	A320-200	737-700	A320-200	737-700	A320-200
W_{fuel}	0.95	0.50	1.81	1.47	3.03	2.86
W_{empty}	-0.29	-0.86	0.02	-0.50	0.75	0.33
TOGW	-0.31	-0.91	0.02	-0.53	0.79	0.35

As the percentage of weight change is compared as the range of the trip is increased, the strut-braced wing decreases in weight in all three categories. The resulting numbers for the weight of the 737-700 and A320-200 are not exactly comparable with the strut-braced design, due to differences in the initial weight. This occurs because the strut-braced design has one extra passenger compared to the 737-700 and two extra passengers compared to the A320-200. This small difference in the input weight is the reason why the strut-braced design weighs more than the other two designs at the shorter ranges. This weight data will be used to derive the estimated costs, noise levels, and aerodynamic characteristics of the Aerohead design.

2.6 Fuselage Design

For the cantilever design concept and the strut-braced wing design concept cylindrical tube fuselages were chosen. The conventional cylindrical tube shape fuselage is the most commonly used and proven shape for a typical 150 passenger aircraft. Its low aerodynamic drag and efficient pressure containing characteristics make it an ideal choice for these two designs. Less material is required to contain an equivalent pressure which in turn reduces the weight of the aircraft.

When designing a fuselage, there are several things that must be taken into consideration, including passenger seating, comfort, and utilities. The RFP requests the aircraft have 150 seats with a dual class seating arrangement with a first class requiring 12 seats at 36” pitch and an economy class requiring 138 seats with 32” pitch. The aircraft should also have a high capacity configuration, meaning the ability to seat a single class with 30” pitch without exit limitations. The cargo capacity should be greater than 7.5 cubic feet. Keeping these criterion in mind and considering examples from other similarly sized passenger aircraft, such as the Boeing 737-800, three cylindrical fuselage designs, were developed, shown in Figures 2.6 and 2.7 on the following pages. Figure 2.6 shows the top view of the passenger seating configurations. A decision to go with the six abreast configuration was made based on the length of fuselage and existing 150 passenger aircraft information. Figure 2.7 shows the front view of the seating configuration that was chosen to provide optimum spacing for passengers and storage. Figure 2.8 displays the exits of the aircraft as well as storage areas on a top-view of the Aerohead design. Two emergency exits are located in the front, two are placed near the middle of the fuselage and two are located in the rear. Two restrooms are located in the rear with an additional one in the front for the first class passengers. Cargo and luggage will be transported on to the aircraft using LD2 containers which will fit in the cargo hold below the main deck, which are further discussed in Section 10.

The blended wing body design concept requires an unconventional fuselage and passenger seating configuration. The fuselage for the blended wing body is not as well defined as the cantilever and strut-braced wing designs. The overall length of this configuration is much shorter than the others. There is also no definitive point where the fuselage meets the wing. The seats must be spread further out from the centerline making the cabin cavity oval in shape. This layout requires a six abreast configuration that spreads into a 10 abreast configuration. An aisle is located through the center with additional aisles on either side for ease of passenger seating. Two emergency exits are placed on the sides of the aircraft in line with the front row of seating. Two exits are also located beneath the wings on either side near the center of the cabin and an additional two are placed in the rear. Figure 2.5, the drawing of the blended wing body shows this configuration. Luggage and cargo will be placed in the aircraft through an opening in the rear.

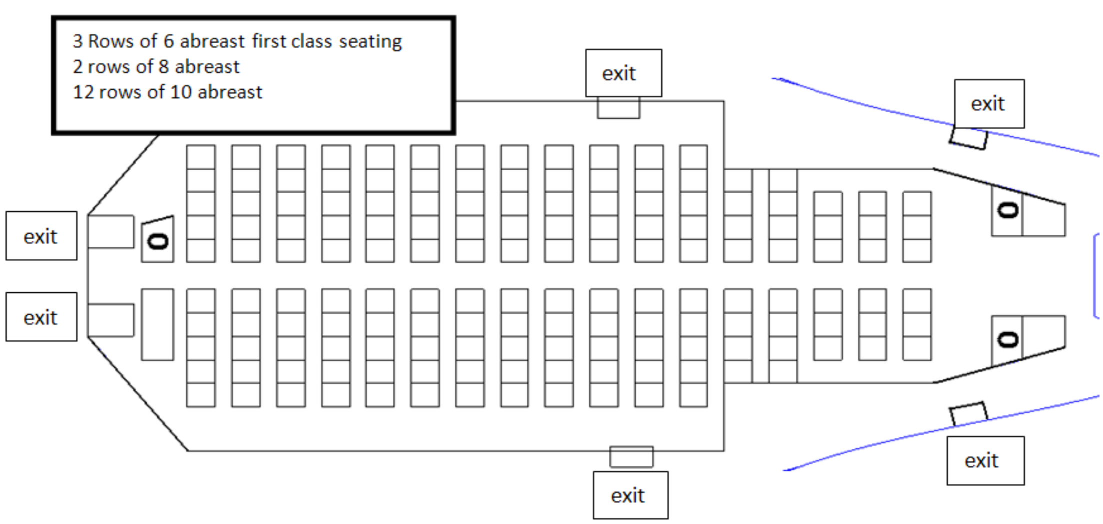

Figure 2.5 BWB seating Configuration

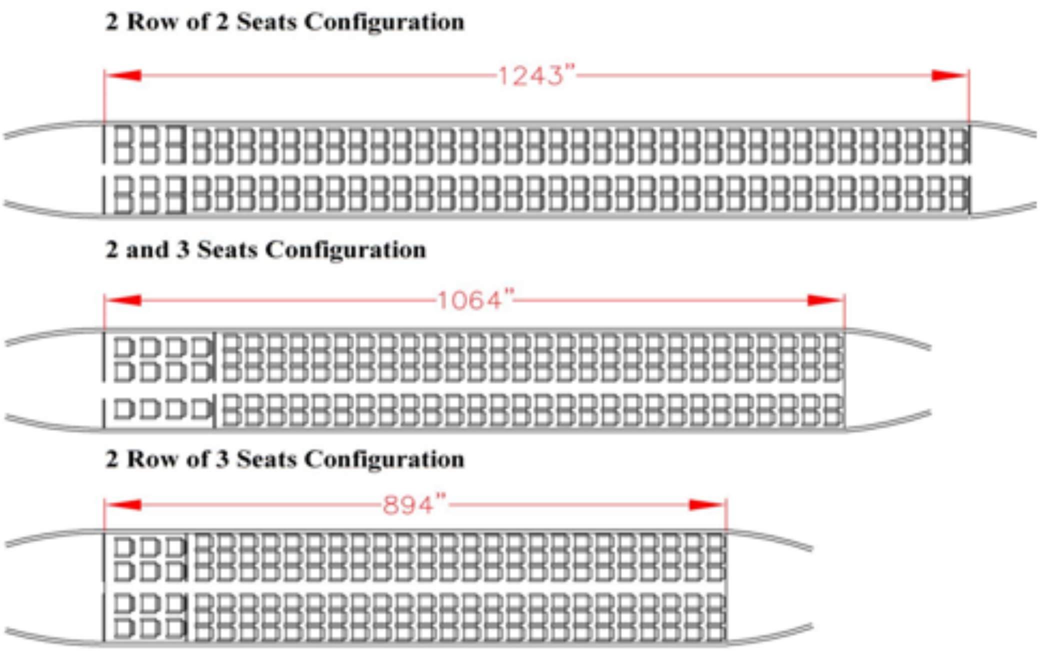

Figure 2.6 Cylindrical Fuselage and Passenger Seating Configuration Layout Designs

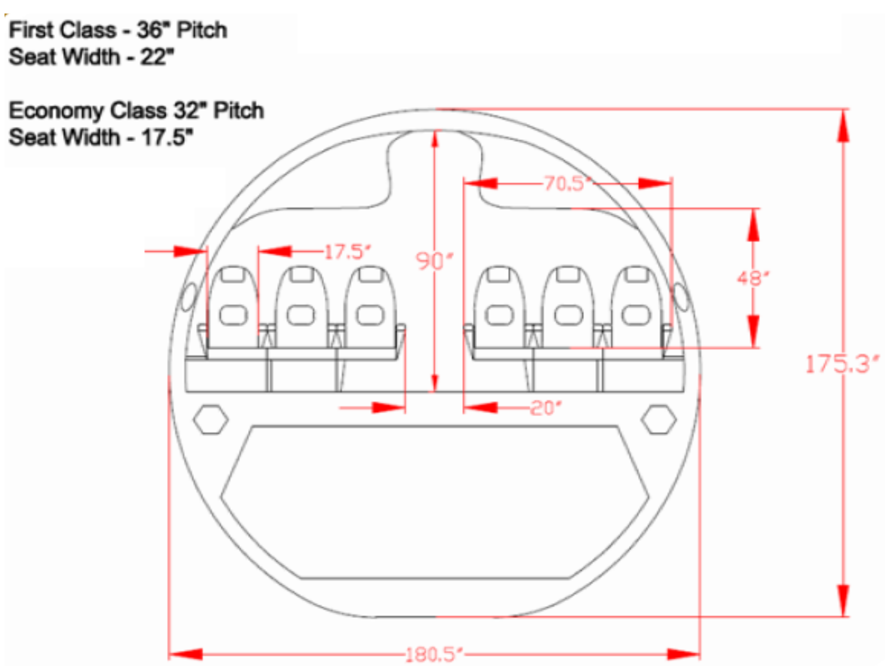

Figure 2.7 Six Abreast Seating Configuration

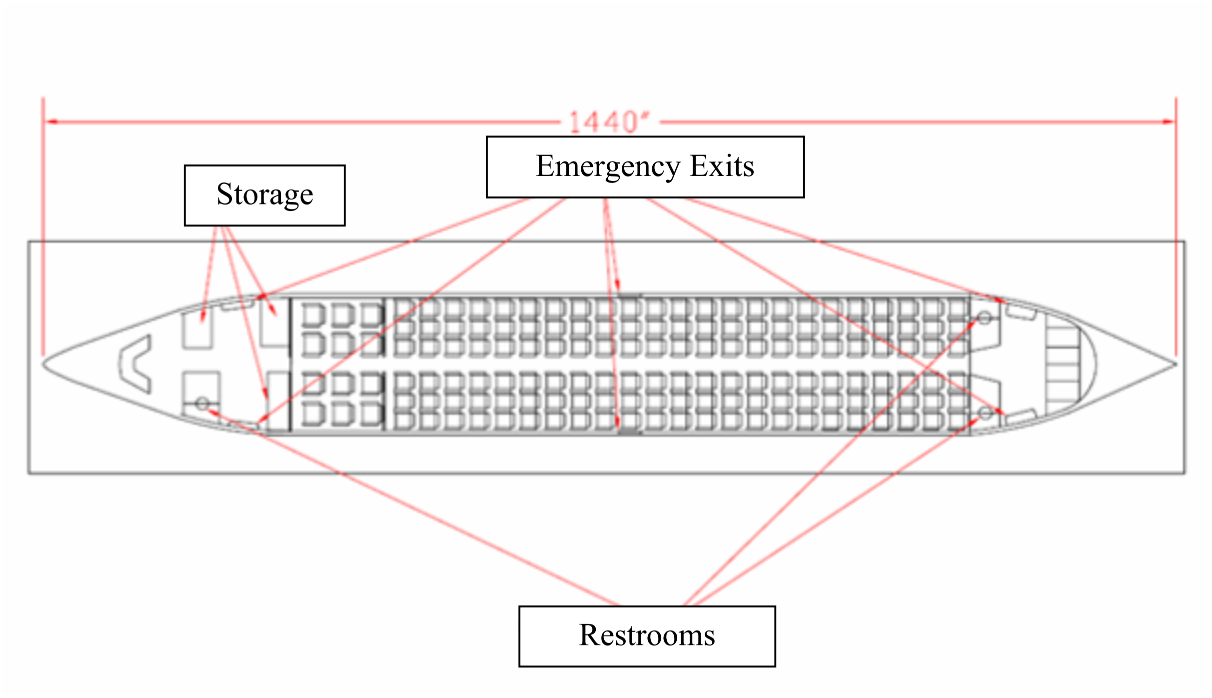

Figure 2.8 Fuselage Exit and Storage Layout

Table 2.8 Pro/Con Chart of Design Configurations

Type of Aircraft	Pro	Con
Cantilever	• Reduced wing box structure with engines below wings • Proven design • Fuselage has low aerodynamic drag	• Wing box will be heavier caused by thicker wing • Technology has outdated this design • Near maximum efficiency of this design
Blended Wing Body	• Lifting surface is extremely large • Decreased fuel consumption from reduced weight • Noise reduction from smooth transition from fuselage to wing and from absence of high lift devices	• Cost increase from structural complexity • The fuselage is not an ideal pressure holding vessel • The main gains are achieved as the size increases, thus causing a large increase in weight and cost
Strut Braced	• Strut reduces the need for extra support in the wing box, allowing the wing to be thinner and have an increased span • Decreased wing sweep caused by a small thickness to chord ratio • Smaller thicknesses will increase drag divergence Mach number and decrease the overall drag • Strut allows for a larger aspect ratio	• Interference drag from strut • Compression and tension of strut during flight creates a buckling issue

After carefully considering the pros and cons of each type of aircraft shown in Table 2.8, the team concluded that the best solution to meet and exceed the RFP is a strut-braced wing design.

2.7 Strut Evolution

The choice of the strut-braced wing required careful consideration was made when choosing the placement of the strut and engine. Five different concepts for the strut-engine integration were made, each of which having their respective benefits and detriments. The first design, shown in Figure 2.9, consists the engine located inboard of the wing, near the fuselage. This concept has excellent engine placement from a control standpoint, with respect to engine-out conditions. If one engine is lost the moment produced by the remaining engine will easily be countered by the flight control system. Unfortunately, the long strut of this configuration results in a much thicker and more expensive strut due to the reinforcement required to prevent buckling.

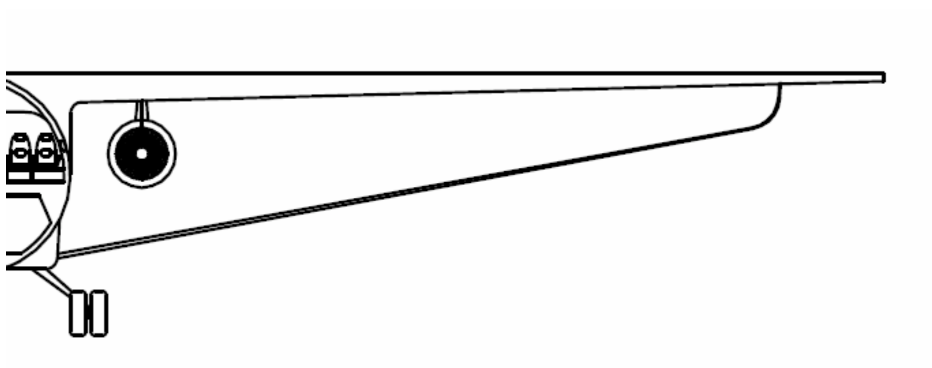

Figure 2.9 Engine Inboard

The next configuration, Figure 2.10, involves the engine directly attached to the strut. This configuration also has a lengthy strut but also places the engine further outboard. This is beneficial from a structural standpoint because the wing no longer requires extra reinforcement to counteract the lifting forces due to the weight of the engine. However, the drag produced by the strut-engine-wing integration is of concern with this configuration. To alleviate this drag, the strut meets the engine nacelle at a 90º angle, eliminating any tight corners that may restrict airflow. Potential buckling of the strut is still a disadvantage of this configuration as well as bending moments produced where the wing meets the engine pylon. In the event of an engine-out, the rudder of the aircraft would have to counter an incredibly large moment due to the distance the engine is placed from the center of gravity.

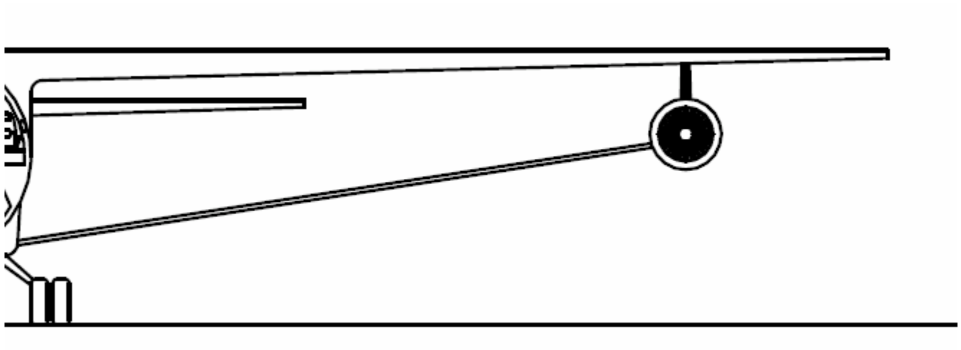

Figure 2.10 Engine Strut Integration

The configuration shown in Figure 2.11 consists of the engine mounted at the mid-span of the wing. This reduces the buckling concern of the strut and aids in the control characteristics of the vehicle. With the engine still located further outboard on the wing, the weight still acts to support the wing spars in countering large lifting forces. The primary drawback of this configuration is the reduced effectiveness of the strut. By placing the strut connection further outboard, the wing loading can be greatly reduced, yet this strut of this configuration only spans half of the wing.

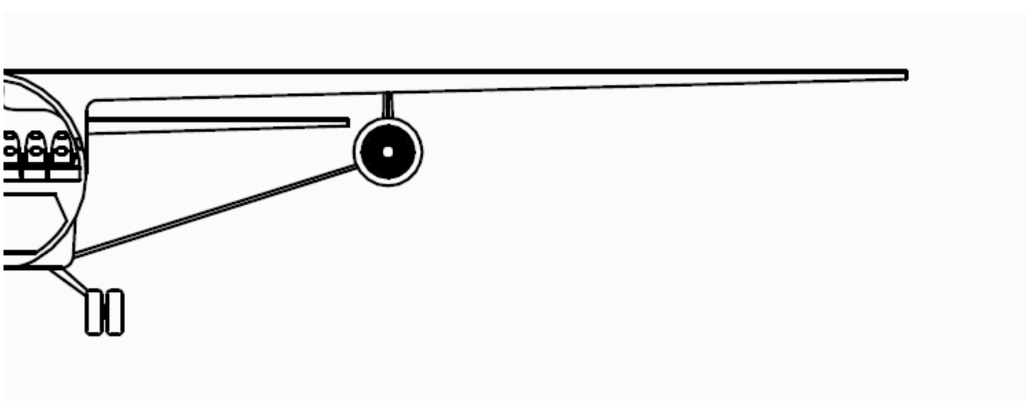

Figure 2.11 Engine Inboard Strut Integration

The configuration shown in Figure 2.12 is an attempt to take all the benefits of each of the previous configurations and combine them into one. The strut reaches out further along the span of the wing alleviating the aircraft wing loading. The engine is placed outboard just enough to maintain flight controls in the event of an engine out without the presence of a large rudder. A jury strut, with the engine mounted in the center, is used to alleviate the buckling concern of the strut. Although this configuration considers several aspects of the wing, it also creates an additional problem: engine maintenance. To remove the engine for routine maintenance or inspection would require a great deal of machinery and disassembly of the jury strut, if not the entire strut. Interference drag produced above and below the engine nacelle would increase due to the sharp corners and small areas between the nacelle and the strut.

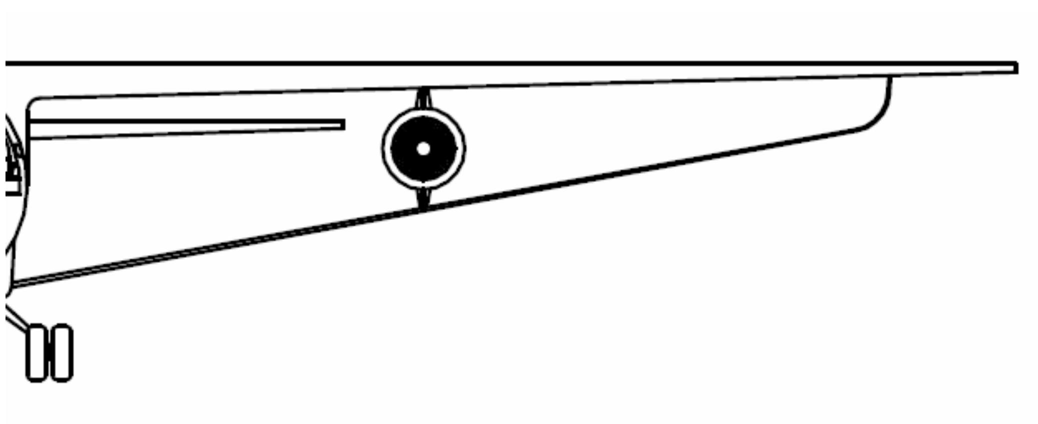

Figure 2.12 Engine Jury Strut Integration

The final configuration, shown in Figure 2.13, alleviates the problem of maintenance difficulties by placing the engine within the strut. The bottom portion of the engine nacelle can be unlatched, permitting the engine to be lowered from its wing mount for any inspection or maintenance. This configuration also eliminates the buckling potential of the strut by decreasing the lengths of the individual members. The overall weight of the wing spar structure is reduced by the engines center of gravity acting on the center span of the wing, not near the fuselage.

However, the engine is still located inboard enough to avoid loss of control in engine out conditions. Lastly, this configuration permits the minimum presence of interference drag by keeping the engine-strut and engine-pylon surface joints at approximately 90º. This large connection angle eliminates any tight spaces that restrict the passage of air that may produce unnecessary drag.

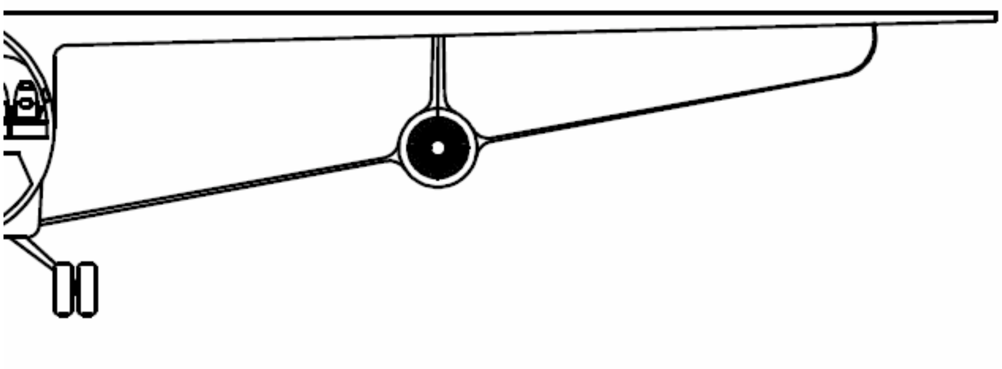

Figure 2.13 Final Configuration- Jury Strut Engine

3. Aerodynamic Analysis

In order to meet the RFP requirements of a long range cruise speed of Mach 0.78 and a maximum cruise altitude of 43,000 feet, a wing that exhibits low drag at cruise speeds and sufficient lift at low speeds must be used. This was accomplished in a number of ways. The strut is the largest contribution to this goal, allowing for a thinner airfoil due to a decrease in wing structure. The decrease in wing thickness allows for a smaller wing sweep. The last aspect of the wing that promotes low drag is a supercritical airfoil. This minimizes the formation of shockwaves and allows the SB-01 to fly at transonic speeds.

3.1 Wing Design

The wing planform was designed based on the thrust to weight versus weight to wing area plot. This required the wing area to be 1699 squared feet, using Figure 3.1 and an aspect ratio of 11, shown by the red star in the figure, giving the wing a span of 136 feet and a mean aerodynamic chord of 12.4 feet.

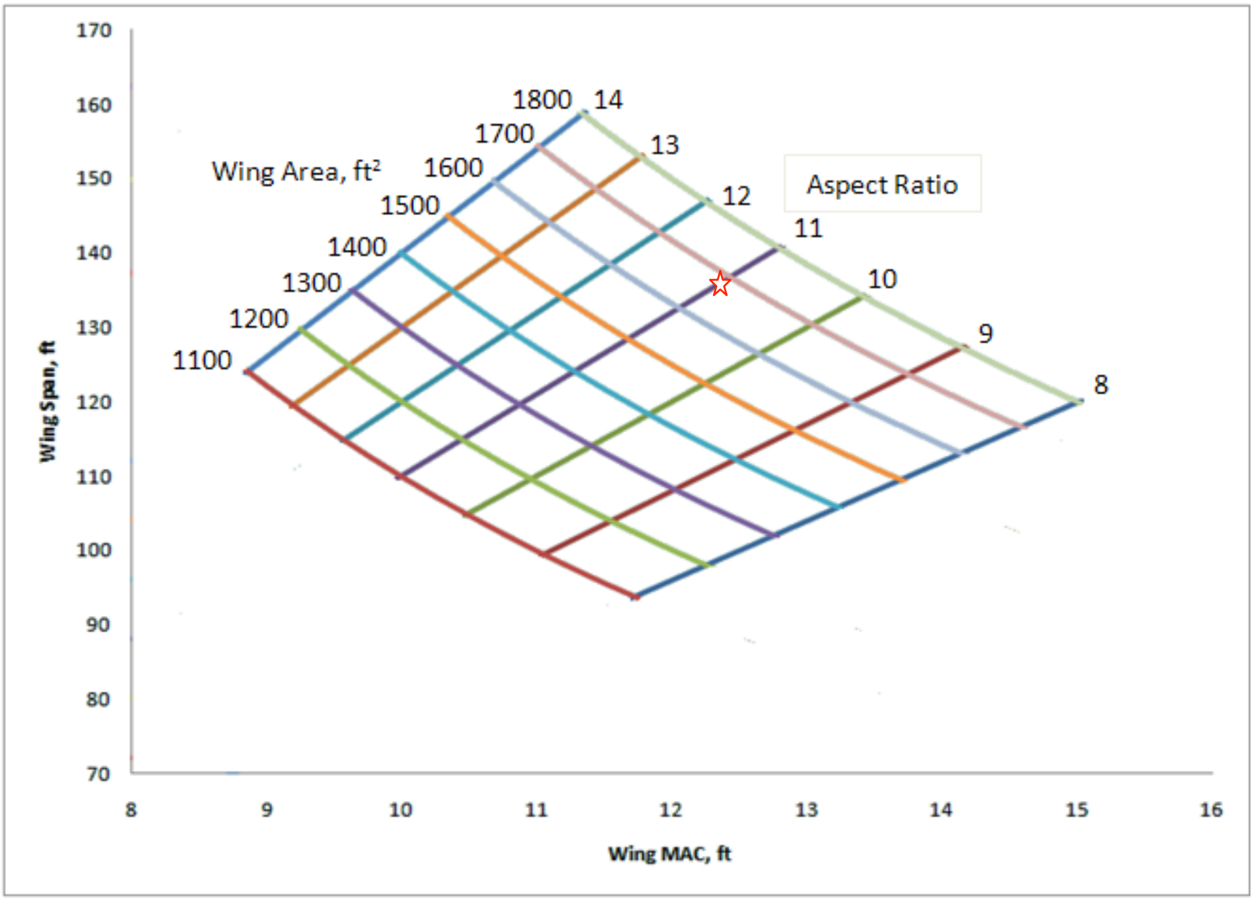

Figure 3.1 Planform Characteristics Carpet Plot

This provided a chord that was small enough to maintain laminar flow over most of the wing. With a cruise Reynolds number of 2.29 x 10^7 it is possible to prevent transition until 80% of the chord, shown as a Reynolds number of 1.8x10^7 in Figure 3.2. Flow along the leading edge, caused by wing sweep, tends to turn the flow over the wing turbulent on longer wings. Lower wing sweep and a smaller chord help to reduce these effects. The last characteristic needed is the taper ratio. A value of 0.25 was chosen in order to have an efficient wing loading.

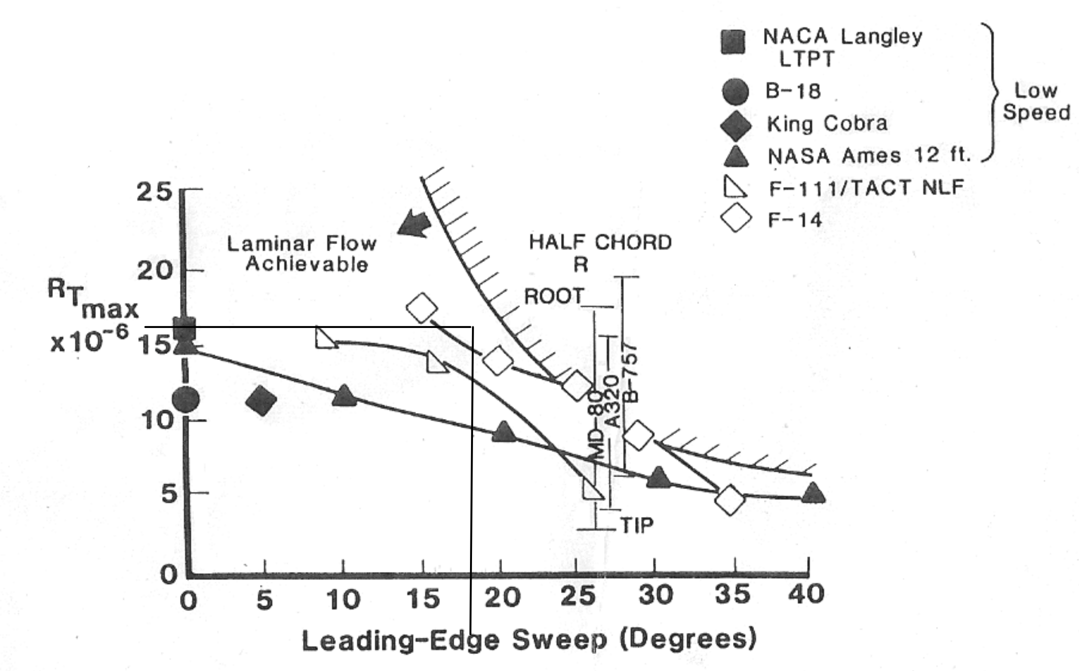

Figure 3.2 Maximum Transition Reynolds Number for Several NLF Experiments

The airfoil thickness and sweep was chosen based on the modified "Korn" equations.

$$???=??\cos(\Lambda)+?/?\cos(\Lambda)2+??10\cos(\Lambda)3 \quad (3.1)$$

It was found that, with a thickness to chord ratio of 0.09 and a quarter chord sweep of 18º, the drag divergence Mach number is around 0.84, well above the maximum cruise speed. From the drag divergence Mach number, the critical Mach number was found to be 0.74, where sonic flow first appears on the wing. From this data, the SC(2)-0709 was chosen. This airfoil, profile shown in Figure 3.3, has a design lift coefficient of 0.7 and a thickness to chord ratio of 0.09.

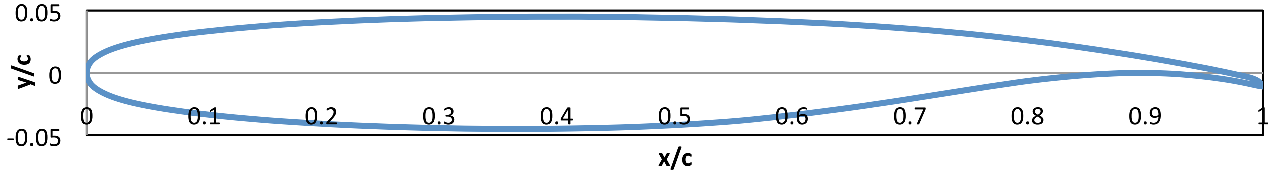

Figure 3.3 SC(2)-0709 Airfoil Profile

This airfoil was then analyzed using *XFoil*. Figure 3.4 shows the lift curve slope of the SC(2)-0709 at sea level conditions and Mach 0.1. It shows that the airfoil will stall at an angle of attack of approximately 16º.

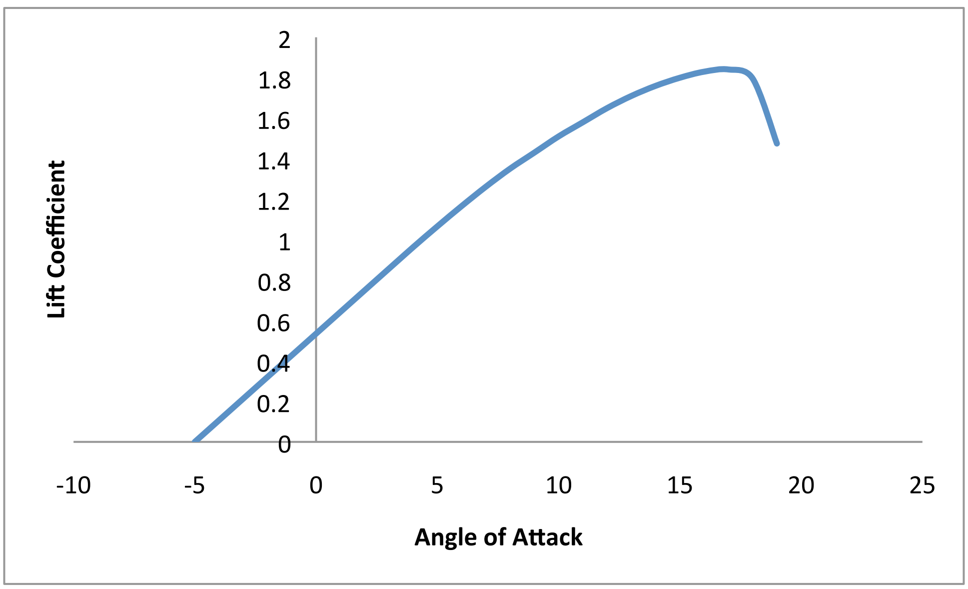

Figure 3.4 Lift Curve for SC(2)-0709

3.2 High Lift Devices

At the low speeds required during takeoff and landing the SB-01 needs additional lift to prevent stall. From the wing loading plots it was determined that a lift coefficient of at least 0.75 is needed for takeoff and a lift coefficient of at least 2.0 is needed for landing. Leading edge slats are employed in order to increase the maximum angle of attack before stall, effectively increasing the maximum lift coefficient by 0.4 at a deflection of around 10º. A set of single slotted flaps are used to produce the rest of the additional lift needed. The flaps on the SB-01 cover 70% of the wing span and 30% of the chord. The flapped area works out to be around 60% of the reference area. When the flaps are deflected at 30º they increase the lift coefficient by 0.64, raising the total lift coefficient to 2.0 at an angle of attack of 5º. Figure 3.5 shows a 2-D depiction of the full high lift system.

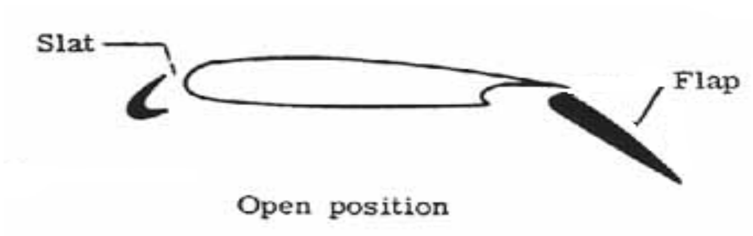

Figure 3.5 High Lift Systems

3.3 Drag Analysis

The drag on the airplane can be separated into three different categories. The first of which is parasite drag. This can be estimated by breaking the plane into its components and using a flat plate estimate. This method is based on the wetted area of each part and includes the effects of roughness, form factor, and pressure drag. The various parts that need to be analyzed for our aircraft are the fuselage, wing, horizontal and vertical tail, strut and landing gear pods. When the plane is taking off and landing the landing gear and high lift devices must also be taken into consideration. The results of this analysis are shown in Figure 3.6, which shows the cruise parasite drag to be around 0.019.

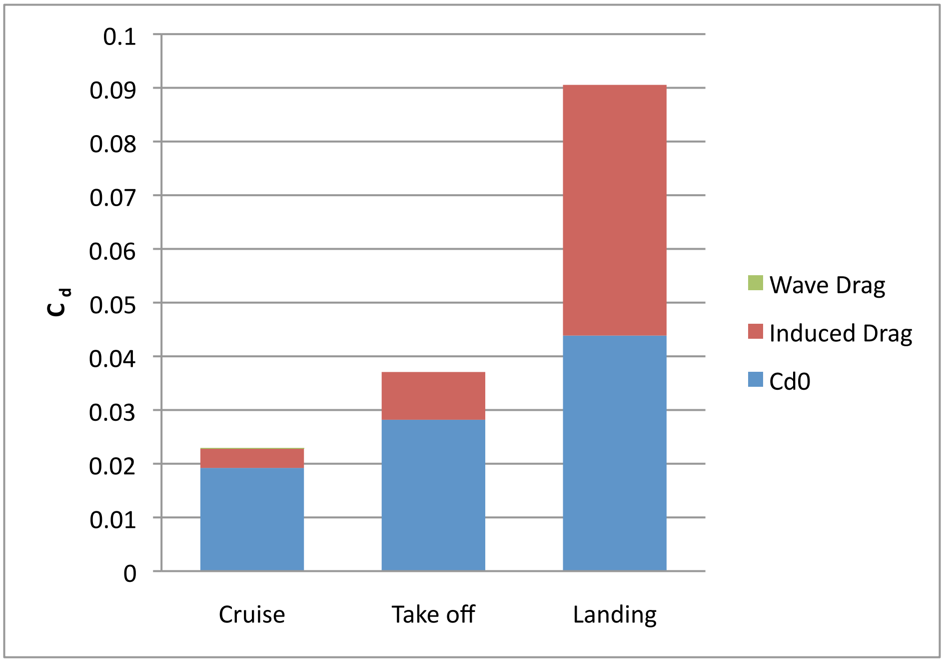

Figure 3.6 Drag Buildup Comparison

The second contribution is the induced drag, due to downwash and lift generated on the wing. This was determined based on the lift coefficient at each flight condition. This type of drag is decreased through the use of a high aspect ratio wing as shown in Figure 3.7.

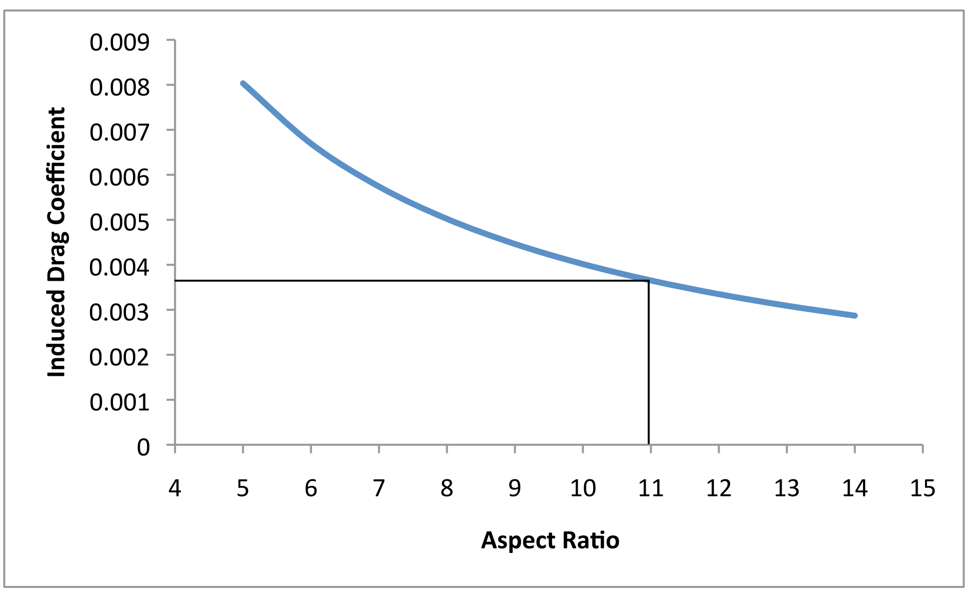

Figure 3.7 Induced Drag versus Aspect Ratio at Cruise

The last form of drag that needs to be considered at transonic speeds is wave drag. Wave drag occurs when shocks appear on the wings and body of the airplane. Wave drag begins when supersonic flow appears on the airfoil, above the critical Mach number. It does not become significant, however, until the drag divergence Mach number is reached. This is shown in Figure 3.8, where a steep rise in drag occurs after Mach 0.84. Figure 3.9 shows the drag characteristics at all three critical stages of flight: cruise, takeoff, and landing.

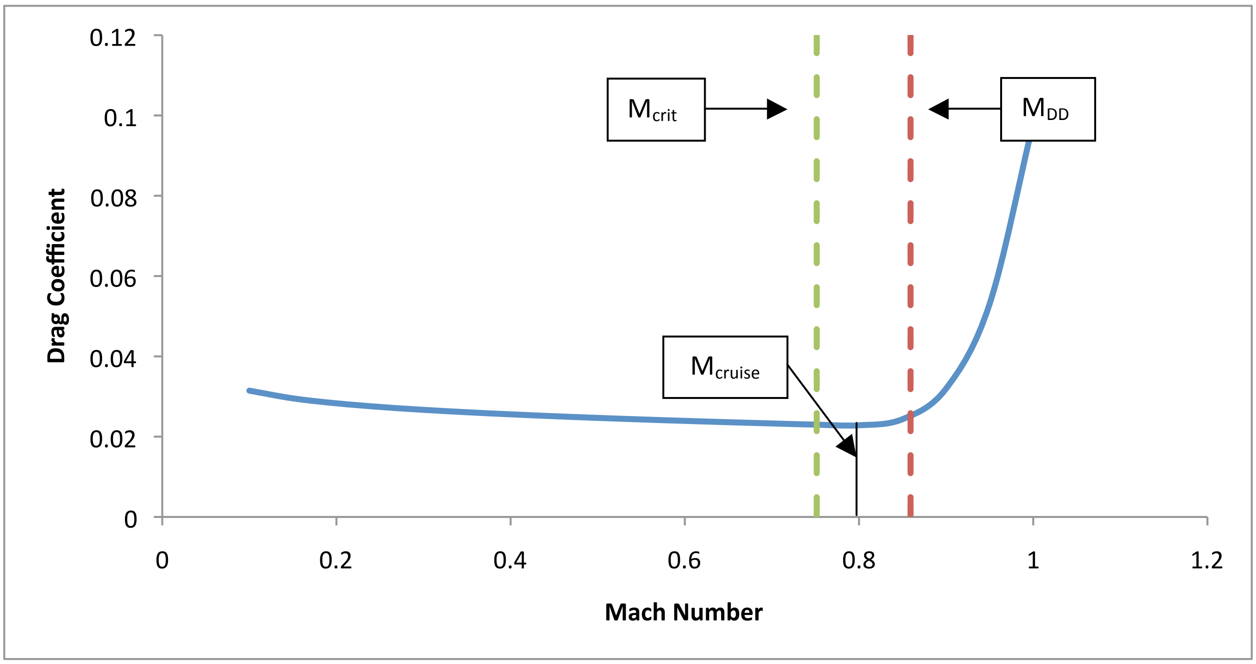

Figure 3.8 Drag Divergence

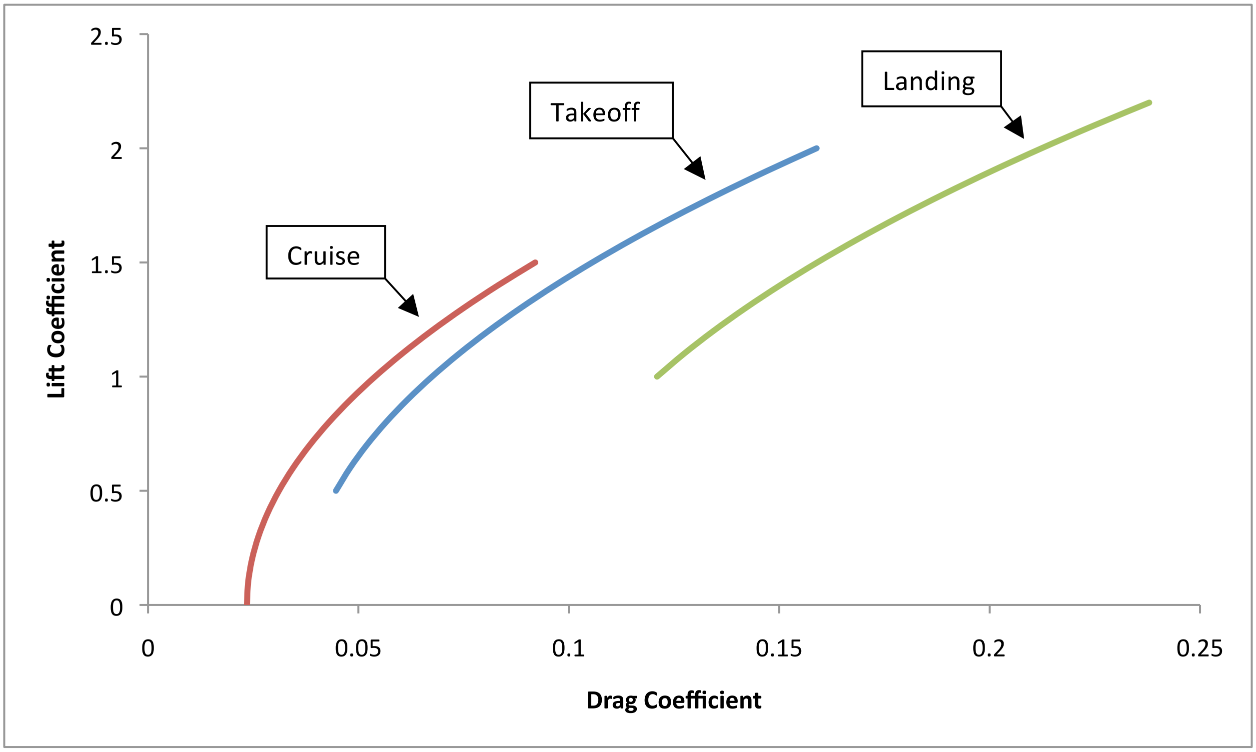

Figure 3.9 Drag Polar

4. Propulsion

The RFP requires a cruise Mach number of 0.78 with a team objective of 0.8. At a range of 500 nm, the airplane should have a maximum fuel burn block ratio of 41 pounds per seat with an objective of 38 pounds per seat. The primary focus includes a reduction in both engine noise and emissions in the form of CO_2, NO_x, and HC. Other engine selection criteria include a simplified design, performance ratings in thrust, higher efficiency with less fuel burn, lower operational and maintenance cost, and reliability. The three engines in consideration include the GE-36, CFM56-7B24, and the PW-1000G. The engine data for each model is shown in Table 4.1.

Table 4.1 Performance Characteristics of Proposed Engines

Engine	GE-36	CMF56-7B24	PW-1000G
Type	Open Rotor	Turbofan	Geared-Turbofan
Thrust (lbs)	25-30% less than current	24,000 lbs	17000-23000 lbs
Cruise SFC	0.27	0.37	0.3256
Bypass Ratio	50.00	5.3	12
Weight (lbs)	5010 lb	5216 lb	less than current
Fan Diameter (in)	120	61	73
Engine Length (in)	N/A	98.9	N/A
Total Emissions:			
HC	much lower emissions than jet engines due to high bypass ratio	69.4% less than ICAO	12% reduce 1,500 lbs per plane per year
CO_2	27% reduction relative to year 2000 engines	61.4% less than ICAO	N/A
No_x	50-60% lower nitrous oxide than CAEP6 2008 standards	39.5% less than ICAO	50% less than CAEP6

4.1 GE-36 Open Rotor

The GE-36 is a modified turbofan engine with the fan placed outside the engine nacelle on the same axis as the compressor blades. The blades have a counter-rotating design that improves the blade efficiency. This engine allows for the plane to move at slower speeds, reducing operating noise. However, vibrations from the blades produce a large amount of noise which nullifies the reduction in noise from slower operating speeds. Testing on the GE-36 shows a 25% improvement in the specific fuel consumption compared to the CFM56-5B3 engine. Tests also show that the engine has a high bypass ratio of 35, resulting in a 25% reduction in thrust compared to single aisle turbofan engines.[5] Despite the reduction in thrust, the GE-36 open rotor engine will provide the same performance and speed as that of a typical turbofan engine.[6]

Figure 4.1. GE- 36 Open Rotor Engine[7]

4.2 CFM56-7B24

In comparison with the CFM56-3 series, the CFM56-7B24 has improved thrust values, improved efficiencies and lower maintenance costs. The engine contains a dual annular combustor with an improved internal design, which allows the engine components to operate more efficiently.[8] The double annular combustor has an inner and outer burning zone where one is always fueled and the other is only fueled during high power settings. This allows the combustor to burn at lower temperatures, which improves the lifespan of the engine components, fuel burn and reduces emissions. The combination of blade casting and a modular design reduces the number of internal components and provides easy maintenance.[9] The reduction in emissions remains the greatest advantage of the CFM56-7B24 turbofan engine.

Figure 4.2 CFM56-7B24 Turbofan Engine[10]

4.3 PW-1000G

The PW-1000G uses a gear box design to allow the fan and turbine to run at their optimal speeds. This allows the fan to operate at slower speeds, which reduces the noise level. The geared turbofan uses ceramic matrix composites to give the engine higher operating temperatures. The low density of the composite materials results in a 50% reduction in the engine weight and a 15% decrease in fuel burn. A simplified design provides the engine with 30% fewer parts and reduced maintenance costs. Other benefits include lower emission taxes and airport landing fees due to a 40% reduction in emissions and lower noise levels.[11] Engine characteristics may improve once final testing is complete and the engine is released into the market.

Figure 4.3 PW1000 G

4.4 Engine Selection

The PW-1000G geared turbofan was selected based on the engine selection criteria and RFP requirements. This engine provides the largest reduction in emission and the lowest operational cost while having comparable thrust values to the GE-36 and the CFM56-7B24. [12]

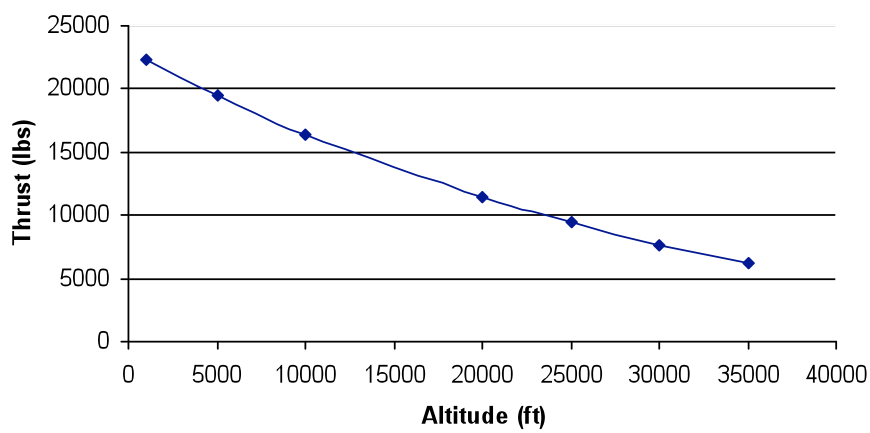

Figure 4.4 Thrust vs. Altitude for PW-1000G

Figure 4.4 shows that the thrust available decreases as the altitude increase, which is a result of decreasing air density with altitude. At a cruise altitude of 35,000 feet, the PW-1000G engine has a thrust available of 6227 pounds. The PW-1000G also fulfills the noise requirement from the RFP by reducing the noise 20 db in comparison to other engines.

4.5 Engine Mounting

The strut-braced configuration of the SB-01 poses an obstacle in terms of engine mounting and accessibility. To maintain the structural integrity of the strut and avoid buckling, the engine mount, shown in Figure 4.4, was designed to absorb the compressive forces produced during landing. The strut will be attached to one of the main bulkheads that is reinforced to absorb the addition loads produced by the strut. Each strut member will meet with the outer rings of the engine nacelle structure. The load will be transferred from the inboard strut to the nacelle structure and then on to the wing tip. As seen in the bottom left portion of Figure 4.5, the bottom section of the structure will contain a hinged door for engine installation and removal. The door of the nacelle requires that the top portion of the nacelle withstand the bulk of the loading that is applied to the engine housing. To maintain the structural integrity, this portion of nacelle with be reinforced with longitudinal stringers.

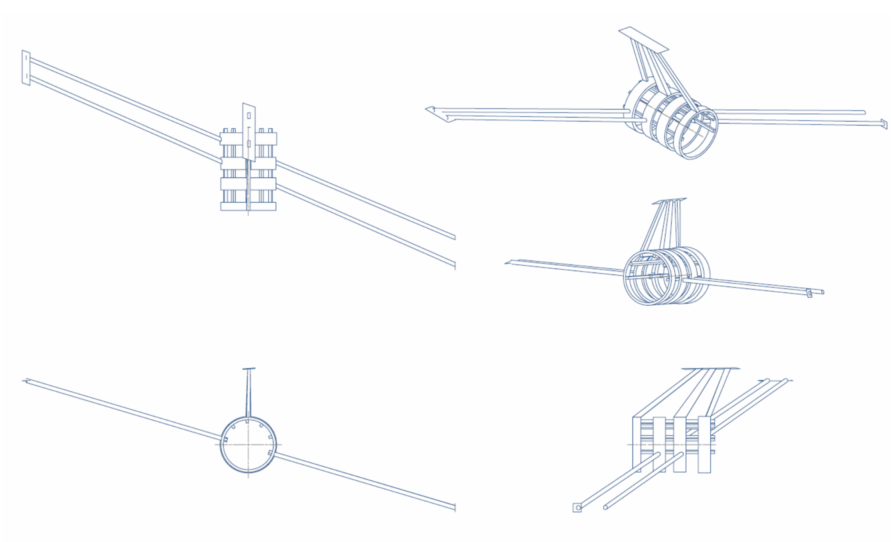

Figure 4.5 Engine Nacelle-Strut Mount

5. Weights

5.1 Final Weights

The weight of the SB-01 was calculated using the estimation techniques in Dr. Jan Roskam's *Airplane Design Part V*[16]. Each component was estimated using the specific eqautions in the text, however actual values were used when available. The eqautions to find the weight of some of the components depended on the total TOGW. This means that an iteration process needed to take place to find the final TOGW. The weight values in the interation process are shown in Table 5.1 and the weight difference from one step to the next are shown in Table 5.2.

Table 5.1 Iteration Process for the TOGW of the SB-01

Iteration Process (lbs)							
	Initial	**1**	**2**	**3**	**4**	**5**	**6**
Gross Weight	123241	128240	129007	129100	129112	129113	129113
Empty Weight	50669	57515	58281	58375	58386	58387	58387
Zero Fuel	87419	94265	95031	95125	95136	95137	95137

Table 5.2 Weight Difference Between each Iteration

Difference of Weight Between Previous and Next Iteration (lbs)						
	Initial to 1	1 to 2	2 to 3	3 to 4	4 to 5	5 to 6
Gross Weight	4999.0969	766.4148	93.3636	11.3578	1.3815	0.1680
Empty Weight	6845.5668	766.4148	93.3636	11.3578	1.3815	0.1680
Zero Fuel	6845.7358	766.4148	93.3636	11.3578	1.3815	0.1680

The intial step value is from the *Nicolai's* aircraft sizing algorithm[13] shown in Table 2.3. A total of six steps were run to find the ideal weight values. This led to the final values for each component effecting the final TOGW, shown in Table 5.3.

Table 5.3 Aircraft Component Weight Breakdown

Component	Weight[14] (lbs)	Fuselage Station (in)	x-Moment (in-lbs)
Luggage	9,000	964	8,674,452
Passengers	27,750	753	20,884,095
Fuselage	13,382	652	8,725,365
Nose Landing Gear	554	168	92,999
Main Landing Gear	3,137	866	2,717,914
Nacelles	1,485	782	1,161,429
Wing	7,574	841	6,369,425
Horizontal Tail	1,303	1,396	1,819,006
Vertical Tail	784	1,412	1,106,986
Strut	842	781	657,218
Engines (2 Total)	8,725	782	6,822,562
Wing Fuel Tanks	25,974	792	20,580,728
Fuel Tank (Below Deck)	7,077	848	6,004,727
Trapped Fuel	925	772	714,256
Flight Control System	1,962	865	1,696,861
Hydraulic & Pneumatic System	1,109	841	932,715
Instrumentation, Avionics, Electronics	1,869	204	381,207
Electrical Systems	3,015	753	2,268,767
AC, Anti-icing	1,562	835	1,303,669
Oxygen System	210	753	158,042
Auxiliary Power Unit	904	1,412	1,275,887
Furnishings	7,901	753	5,945,820
Fuel System	1,208	841	1,016,001
Propulsion System	863	782	674,519
Gross Weight	**129,113**	**796**	**102,781,696**
Empty Weight	**57,834**	**793**	**45,842,861**
Zero Fuel Weight	**95,137**	**781**	**74,334,040**

The breakdown of the weights are compared to existing aircraft in Table 5.4.

Table 5.4 Weight Comparison of SB-01 to 737-700 and A320-200

Weight	SB-01	737-700	A320-200
Gross Weight	129,113	154,500	170,000
Empty Weight	58,387	84,100	93,000
Zero Fuel	95,137	110,035	119,293

5.2 Center of Gravity

The center of gravity location was calculated using the full list of components that affects the TOGW by summing the moments of each component about the tip of the plane and dividing by the TOGW. The center of gravity was calculated for four different cases, each case is for a different distance traveled: 500, 1000, 2000, and 2800 nm. The center of gravity location will change based on the fuel weight, shown in Table 5.5.

Table 5.5 Center of Gravity Distance for each Mission Range

Distance From Tip of Plane (in)				
	500 nm	**1000 nm**	**2000 nm**	**2800 nm**
With Fuel	792.514	792.508	792.493	796.059
Without Fuel	792.664	792.664	792.664	792.664
Empty Weight	781.333	781.333	781.333	781.333

This is further broken down into the % MAC and distance along the MAC, shown in Tables 5.6 ans 5.7.

Table 5.6 Center of Gravity in Percent of MAC

Percent MAC				
	500 nm	**1000 nm**	**2000 nm**	**2800 nm**
With Fuel	19.610	19.606	19.598	21.741
Without Fuel	19.700	19.700	19.700	19.700
Empty Weight	12.887	12.887	12.887	12.887

Table 5.7 Distance to Center of Gravity along the MAC

Distance Along MAC (in)				
	500 nm	**1000 nm**	**2000 nm**	**2800 nm**
With Fuel	32.615	32.609	32.595	36.160
Without Fuel	32.765	32.765	32.765	32.765
Empty Weight	21.434	21.434	21.434	21.434

6. Aircraft Performance

In order to comply with the AIAA 2009 RFP, the Aerohead design had to meet the performance requirements discussed in the introduction. These specifications included a takeoff field length no greater than 7000 feet at sea level at 86º F, a maximum landing speed of 135 knots, maximum range of 2800 nautical miles with a full dual class passenger load, and a cruise speed no less than 0.78 Mach at 35,000 feet + 15ºC. In order to thoroughly analyze the performance of the Aerohead SB-01, several equations and processes were utilized from Roskam's *Airplane Design Part VII*[17].

6.1 Takeoff and Landing

As required for all commercial airliners, the SB-01 is subject to FAR 25 requirements, meaning it must be capable of clearing a 35-foot obstacle at decision speed in the event of an engine failure on a dry runway surface. Assuming the runway is constructed from concrete and asphalt and the air density at 86ºF is 0.002354 slugs/ft^3; equations provided by Roskam[5] were used to determine the takeoff characteristics of the SB-01. The take off field length is 3857 feet with a takeoff ground run of 2778 feet based upon a stall speed of 105.88 knots. The balanced field length of the aircraft is 4948 feet which is well below the RFP required 7000 feet.

Landing calculations were performed using the same reference beginning with an approach speed of 1.3Vstall, specifically 137.65 knots, involving the additional obstacle clearance of a 50 foot object is required. The approach distance of 1338.13 feet leads to an additional landing ground run distance of 1371.5 feet. The overall landing field length is 4516 feet. The final landing velocity of the SB-01 is 130.6 knots, coming in right below the maximum landing velocity stated by the RFP. The total landing field length of the Aerohead SB-01 at maximum landing weight is 4516 feet, which is 2% smaller than that of the Boeing 737-300 and 6% smaller than the Airbus A320-200.[18]

6.2 Range and Altitude Requirements

The RFP requires a maximum range of 2800 nautical miles at maximum capacity to suffice for the variety of missions that the SB-01 is required to complete. Although Pratt and Whitney have not disclosed the actual specific fuel consumption of the PW1000G engines, they have stated that it shows a 12% improvement over the 0.37 lb/lbf-h of the CFM56-7B turbofan so an estimated fuel burn was calculated to be 0.3256 lb/lbf-h. Combining the proposed SFC with the Breguet range equation[1] and confirming by Roskam's[17] methods, the SB-01 is capable of missions up to a range of 3024 nautical miles with an endurance of 7.26 hours, clearly exceeding the specifications set forth by the RFP.

The Aerohead design has a maximum rate of climb of 4061 feet per minute and can climb to a cruising altitude of 35,000 feet in 8.62 minutes at an angle of 11.31°. In a reverse fashion, an absolute ceiling altitude of 43,500 feet is obtained by setting the climb rate to only 500 feet per minute. At the cruise altitude, the SB-01 is capable of travelling at a maximum speed of 0.9 Mach due to the amount of thrust produced by the PW1000G engines. The stall and maximum speeds are shown on the thrust curves below and indicate the aircraft satisfies the RFP. The graph shown in Figure 6.1 shows the required thrust for flight at 35,000 feet and the thrust available from the PW1000G engines. The intersection of these lines at Mach 0.90 is the maximum operating speed of the SB-01 at 35,000 feet, which is well above the required Mach 0.80.

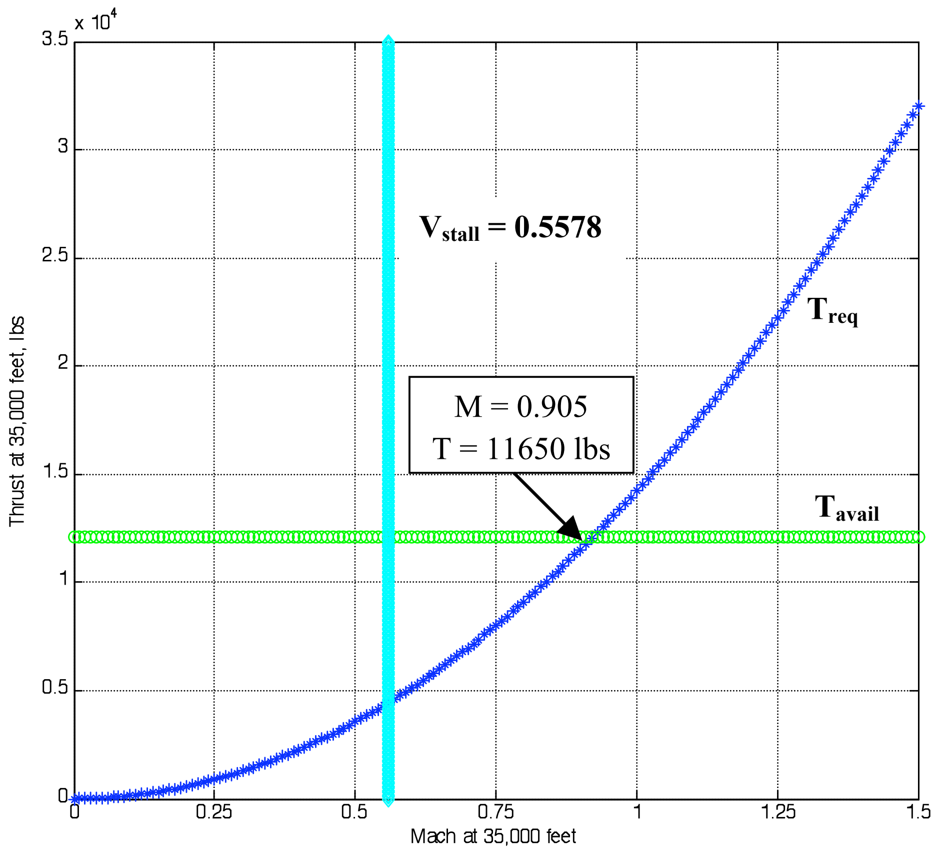

Figure 6.1 Thrust Curve for Aerohead SB-01

Following Roskam's Aircraft Performance guide[17], a mission profile was constructed for the SB-01 shown in Figure 6.2.

Aerohead SB-01 Commercial Airliner

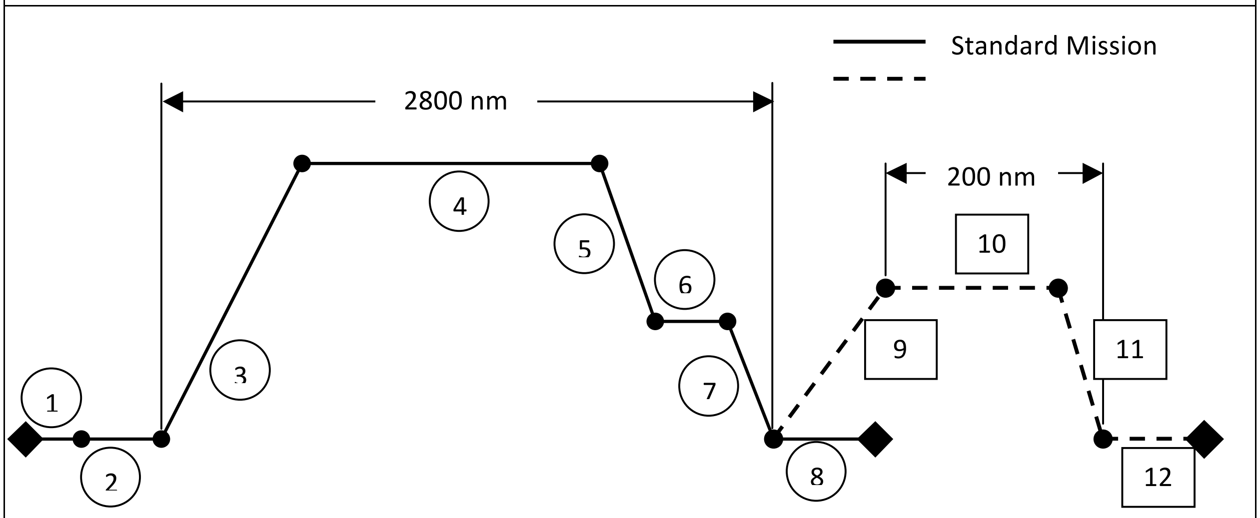

TOGW – 129,113 LB WT @ 50% FUEL – 112,125 LB WT @ 75% FUEL – 120,619 LB	TAKEOFF DISTANCE – 4950 FT (BFL) LANDING DISTANCE – 4516 FT

Mission Segment	Mach	Altitude (ft)	Time (min)	Fuel (lb)	Distance (nm)
1. Warm up and Taxi	0	0	15.00	950	0.00
2. Takeoff	0 – 0.3	0	1.50	4512	0.82
3. Climb to Cruise	0.3 – 0.78	35,000	8.75	6950	30.00
4. Cruise	0.78	35,000	364.13	14064	2729.00
5. Initial Descent	0.78 – 0.6	10,000	4.25	-	25.00
6. Loiter	0.6	10,000	1.75	926	10.00
7. Final Descent	0.6 – 0.2	0	1.00	-	5.00
8. Land	0.2 – 0	0	0.60	663	0.74
9. Climb to Reroute Altitude	0.2 – 0.6	15,000	4.57	3584	6.75
10. Cruise to Alternate	0.6	15,000	30.00	1739	188.00
11. Descend to Sea Level	0.6 – 0.2	0	2.00	-	5.25
12. Land	0	0	0.60	663	0.74
Total	**-**	**-**	**434.15**	**34051**	**3001.3**

Figure 6.2 Mission Profile of Aerohead Aeronautics SB-01 Commercial Airliner

7. Noise Reduction

As today's National Airspace (NAS) becomes heavily populated with air travel and the abundance of noise propagation coming from many aircraft it is necessary to implement noise reduction techniques for airplanes. To meet RFP requirements, of which is -20dB cumulative noise reduction from ICAO (International Civil Aviation Organization) Chapter 4 regulations or ICAO Chapter 3 minus 30dB from three noise profiles. Three profiles that contribute to noise compilation are lateral flight, fly-over flight, and approach flight. The biggest proponent of noise reduction of the SB-01 is the ability to reduce flyover and approach flight noise additions from aircraft structure.

In the cases of the three conceptual designs the following calculations were made for Chapter 4 requirements based on the weight of the aircraft. Using the following equations estimated noise values were found for each of the three profiles; fly-over noise is calculated with the constraint of having only two engines.

$$\text{Lateral Noise: } 80.87+8.5\text{LOG}(W) \tag{7.1}$$

$$\text{Fly-over Noise: } 66.95+13.29\text{LOG}(W) \tag{7.2}$$

$$\text{Approach Noise: } 86.03+7.75\text{LOG}(W) \tag{7.3}$$

Table 7.1 shows that the strut-braced design has the lowest weight which results in the lowest noise estimation. These values however are not taking into account the cumulative distribution to meet the -20 dB requirement.

Table 7.1 Estimated Noise Levels based on Aircraft Weight

	Weight (lbs)	Sideline Noise (dB):	Fly-Over Noise (dB):	Approach Noise (dB):
SB-01	129,113	91.55	89.29	94.95

The engine that will be operating the SB-01 is the Pratt and Whitney Pure Power 1000G turbo fan. This engine will reduce fuel burn, emissions, engine noise, and operating costs. The PW 1000G has a promise of reducing noise by 20dB which will aid in the reduction of noise on lateral flight and fly-over flight. This reduction alone meets RFP requirements. However this is only an estimate and further analysis is needed.

Recently research has been done to reduce airframe noise, including reducing noise from the landing gear. This is due to landing approach airframe noise contributing to half of the noise perceived when the engine is operating at low thrusts. To minimize this, Aerohead Aeronautics has introduced a strut-braced wing concept to maximize lift and minimize drag, reducing the need for high lift devices. This will aid in the ability to keep airframe noise down. The other main issue for airframe noise is the landing gear (Accounts for roughly 40% of airframe noise [20]). The following explains how Aerohead Aeronautics plans to attack this issue. The upper leg area, the steering system and the tow-bar contribute most of the aerodynamic noise perceived. [20] To reduce these effects the SB-01 nose landing gear, as seen in Figure 7.1, has spoilers to protect the upper gear area from high speed flow and an inverted steering mechanism that is located in the bay of the plane. Also the tow-bar is turned around so that it is behind the wake of the landing gear.[20] The lights are not a part of the landing gear but in the bay and also the outer hubcaps are plugged so that there is a smooth surface so air flow does not interact with them. The main landing gear, seen in Figure 7.2, has fairings attached to protect the forward parts and brakes from the flow. A study performed at Virginia Tech indicates that this will aid in the reduction of noise by -6dB.[21] The bogey system in the main landing gear has a bogey beam under tray which reduces the interaction of the incoming flow with the area where the wheels are connected to the strut.

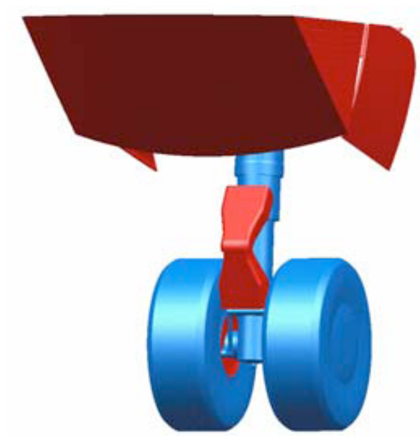

Figure 7.1 Nose Landing Gear Assembly with Spoiler Cover [20]

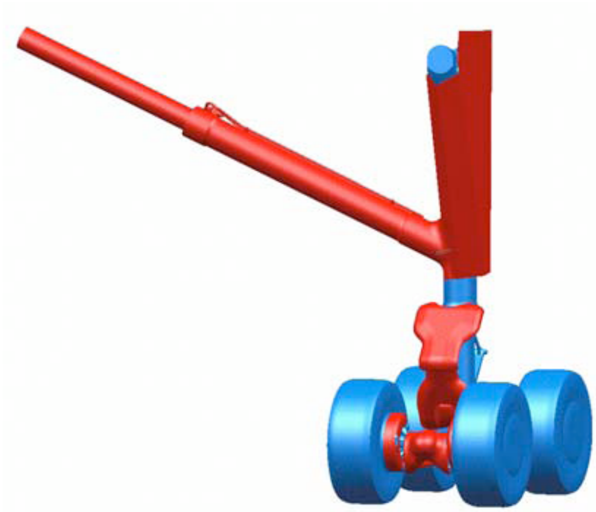

Figure 7.2 Main Landing Gear Assembly with Fairings [20]

The SB-01 will meet RFP design criteria for -20 db cumulative with the Pratt and Whitney 1000G engine and the reduction in airframe noise, the aircraft will have less noise than that of any aircraft today. This is because the engine reduces noise with a high by pass ratio engine that reduces noise by 20 dB alone. The landing gear installation will reduce noise by -6 dB with proper fairings and spoilers.

8. Structures

The SB-01 is constructed from a wide variety of materials to uphold the structural integrity when subjected to the forces of flight. A key feature of the Aerohead design is the use of new composite materials that maintain the strength of the structure yet reduce the weight. These weight savings allot room for additional control and environmental systems while reducing the overall TOGW of the vehicle. Although the configuration of the strut-braced design is not too different than a conventional design, the extended wing span and strut assembly rely on incredibly high-strength supports and joints.

8.1 V-n Diagram Section

In order to determine the structure needed for the SB-01, the loads on the aircraft must be determined. The V-n diagram, seen in Figure 8.1, was created in order to understand the maneuvering limit loads including loads under gust conditions. This diagram was made in accordance with the Military Specification 1-8861b[47], stating that transport aircraft must have a limit load factors of 2.5 and -1.

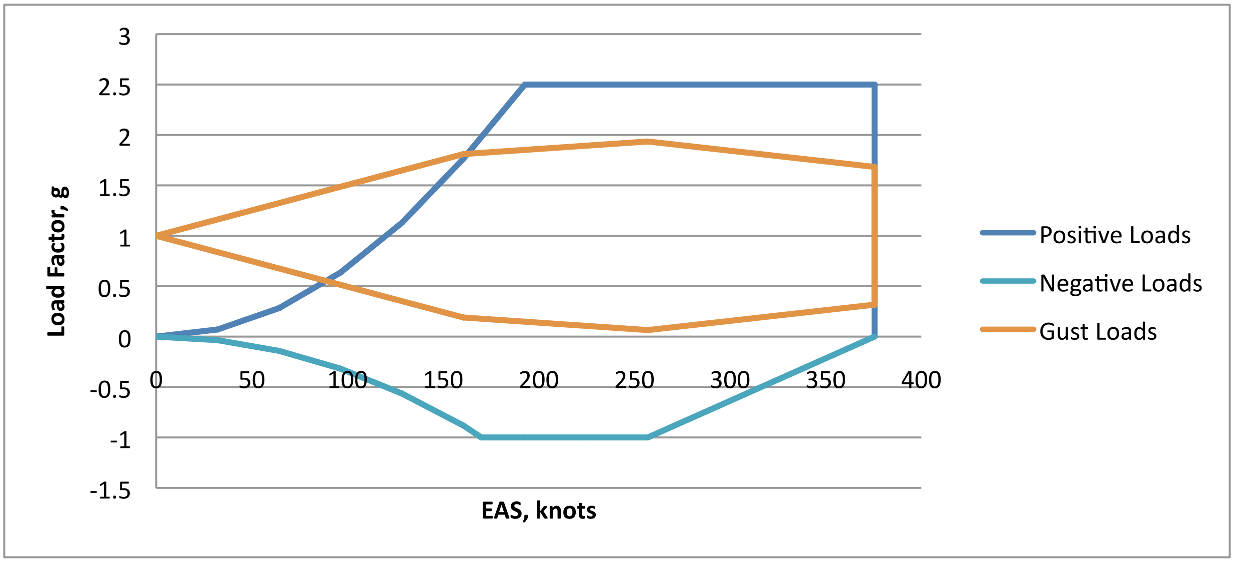

Figure 8.1 V-n Diagram

8.2 Wing Box

The wing box of the SB-01 is constructed from carbon fiber reinforced plastic (CFRP) which is far superior to the aluminum and titanium alloy boxes utilized today. The material consists of a graphite epoxy formed on layers of woven carbon, aluminum, or aramid fibers.[22] The weave of these fibers ranges from unidirectional, to support loads that act in only one direction, to multi-directional, to support loads that act in several directions. Although temperature limitations prohibit the use of CFRP on high-speed vehicles, the use on commercial airliners that travel in only the transonic regime is unaffected. CFRP offers a much larger yield strength to density ratio as well as fracture toughness than both aluminum and titanium alloys, as shown with additional materials in Table 8.1.[23] A high strength to density ratio assures that the main wing structure will not only support the multitude of loads acting on the extended wing of the strut-braced design but also minimize the weight to produce an efficient aircraft. The immense fracture toughness offered by the graphite-epoxy-based material is vital to the structure of the wing box because it prohibits the propagation of any initial cracks that could lead to

catastrophic failure. Additionally, CFRP is incredibly resistant to corrosion of both salt and fresh water. The SB-01 wing is connected to the fuselage by an AMS 4914 titanium alloy discussed in Section 2.3. The attributes of this composite reduce the need for excessive maintenance, cleaning, or replacement and correspondingly reduce the overall life cycle cost of the aircraft. The wing box of the Boeing 787 has already been constructed from CFRP and the material is continuing to be used across the aeronautics industry.[24]

8.3 Control Surfaces

The SB-01 control surfaces are primarily constructed from an aluminum 2024-T0 alloy and are covered with the GKN heating mats described in Section 10.7. This alloy has moderate strength yet is incredibly cheap in comparison to the CFRP. The 2024-T0 alloy features a high thermal conductivity useful for de-icing the control surfaces and is of reasonable density as to not add to the aircraft weight. The use of aluminum for the leading edges of the wings permits easy and inexpensive repair in the event of bird strikes. Although a composite leading edge would possess higher strength and toughness, any actual damage to the surface would require entire replacement as CFRP material does not repair easily.

8.4 Strut

The strut of the Aerohead design is also constructed on a CFRP wing box due to the strength characteristics with aluminum alloy leading edges. The strut provides support for the extended wing as well as restricts upward deflection during flight, a task normally performed by the wing box. The SB-01 also incorporates the strut into the nacelle to distribute the possible buckling loads that are experienced upon landing. A single strut running from fuselage to wing is subjected to enormous downward loads that may cause the support to buckle. However, by breaking the strut into two sections and adding a jury-strut to the engine, the downward force is

redistributed throughout the strut assembly alleviating any enormous force. The strut is attached to the fuselage at the foremost landing gear bulkhead by the combination of a 7075-T0 aluminum alloy and an AMS 4914 titanium alloy. This alloy combination is also utilized to attach the strut to the engine nacelles as well as the wing. This titanium alloy is incredibly strong and carries the majority of the load while additional joining members are constructed from the aluminum, again to minimize weight.

8.5 Engine Nacelle

The twin PW1000G engines are housed in a fiber metal laminate (FML) nacelle. The size and power of these engines require that the surrounding material be capable of withstanding immense heat as well as exhibit high strength. Specifically, GLARE will be used due to its high resistance to corrosion, fire, and impact damage. GLARE is composed of several layers of aluminum bonded together by epoxy with woven glass fibers in between.[25] This material is much lighter than aluminum alloys and is currently being installed on the Airbus A380 as well as the C-17 *Globemaster III*. The nacelles will be attached to the wing and strut by an AMS 4914 titanium alloy.

8.6 Aircraft Skin

The skin of the Aerohead SB-01 is primarily composed of CFRP with the exception of the nose cone, landing gear pods, and wing-fuselage intersection. Although the nose cone is constructed from fiber-glass to allow the radar to perform properly, the remainder of the aircraft is constructed from CFRP on an aluminum alloy frame. The composite skin of the aircraft, although pricey, yields a vast reduction in structural weight compared to the conventional 2024-T0 aluminum skin, or the outdated duralumin. The fuselage-wing intersection does not require high-strength protection due to the amount of titanium alloy fasteners that are already present so this region will also be enclosed in fiber-glass.

8.7 Landing Gear

The landing gear of the SB-01 protrudes from the lower sides of the fuselage and is housed in fiberglass pods. Although the structural strength of the gear depends on the titanium alloy used to fasten the gear assembly to the corresponding bulkhead, the pod material does not require excessive strength. The landing gear struts are composed of 7075-T0 aluminum alloy that are reinforced with AF1410 high alloy steel. Titanium alpha-beta alloy is also used due to its strength and corrosion resistance.

8.8 Manufacturing

Although Table 8.1 shows that CFRP is much more expensive than the 2024-T0 and 7075-T0 aluminum alloys, its manufacturability suggests that it is a wiser choice. CFRP can be molded into a variety of shapes with ease and very little material, if any, is considered waste. The forming and setting of composites requires much more time in terms of component production yet advances have shown that the process is more efficient than metal sculpting. The shaping and forming of structural members from aluminum requires a wide variety of machining equipment. The excessive drilling and carving of the aluminum produces an incredible amount of waste that gradually ends up as scrap metal and does not get used. Titanium alloys require temperatures over 1000°F to form and are vulnerable to impurities that may cause defects or brittleness. As more metals are introduced into the world of composites, the methods of manufacturing composites into aerospace applications are becoming even less challenging.

Table 8.1 Table of Material Properties for Aerohead SB-01[23]

Parameter	Al Alloy 2024-T0	Al Alloy 7075-T0	AF1410 Steel	CFRP	Ti Alloy AMS 4914	Ti-6A-4V Annealed
Cost ($/kg)	2.83	2.74	11.9	56.8	84.55	2.74
Density (kg/m^3)	2.77×10^3	2.8×10^3	7.83×10^3	1.58×10^3	4.76×10^3	2.8×10^3
Yield Strength (Pa)	7.5×10^7	1.05×10^8	1.56×10^9	5.5×10^8	7.61×10^8	1.05×10^8
Compressive Strength (Pa)	7.5×10^7	1.05×10^8	1.64×10^9	5.69×10^8	7.63×10^8	1.05×10^8
Fracture Toughness ($Pa\text{-}m^{1/2}$)	3.8×10^7	3.7×10^7	1.55×10^8	4.69×10^8	6.25×10^7	3.7×10^7
Fatigue Strength at 10^7 Cycles (Pa)	4.1×10^7	5.16×10^7	7.0×10^8	3.35×10^8	5.0×10^8	5.16×10^7
Vickers Hardness (Pa)	5.4×10^8	3.24×10^8	5.39×10^9	1.59×10^8	2.24×10^9	3.24×10^8
Thermal Conductivity (W/m-K)	193	134	29.15	1.64	8.1	134
Corrosion	-	-	-	-	-	-
Fresh Water	Very Good	Very Good	Good	Very Good	Very Good	Very Good
Salt Water	Good	Good	Average	Very Good	Very Good	Good
Sunlight (UV radiation)	Very Good	Very Good	Very Good	Good	Very Good	Very Good

8.9 Structural Overview

The incorporation of the strut to the conventional modern airframe required careful analysis of bulkheads as well as longerons and stringers. By analyzing existing airframes and considering new technologies, the Aerohead SB-01 structure was determined as discussed below.

Figure 8.2 shows the basic structural layout of the Aerohead design. Designated in red are the main load paths of the structure. Loads on the wing the air are transferred from the outer skin of the structure to the stringers, bulkheads, and spars. The fuselage is of semi-monocoque

construction. The main cylindrical fuselage will contain longitudinal elements (longerons and stringers), transverse elements (frames and bulkheads), as well as its external skin. Longerons and stringers will carry axial loads from bending moments while the skin will carry shear and pressure force loads. Heavy bulkheads near the wing attachment points serve to distribute the concentrated forces from the landing gear, strut, and wing. Skin thickness will be generally thicker on the wing due to the greater amount of pressure loads applied along the surface. The semi-monocoque frame of the SB-01 will withstand the numerous forces encountered during flight. It has a very high strength to weight ratio and has proven itself throughout the commercial industry to withstand unusual load combinations and locations.

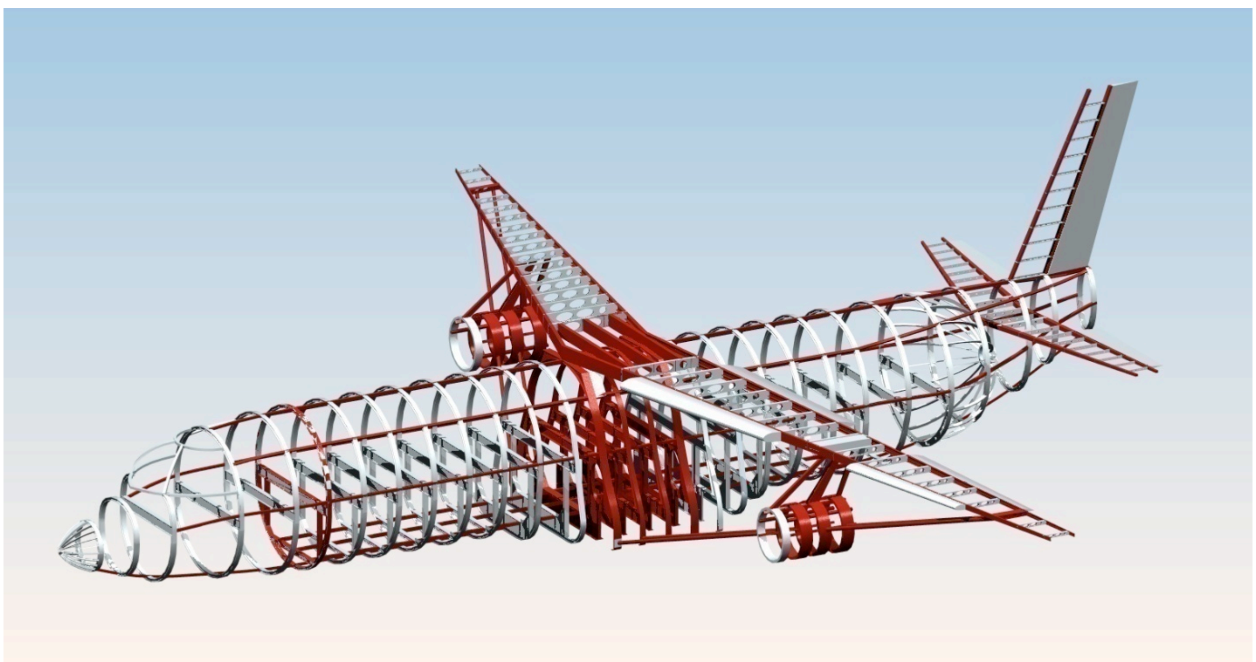

Figure 8.2 Load-bearing members of SB-01

The majority of the lightweight rib frames will be placed at 36” apart. However, near the wing spar attachment, they will be placed 24” apart for greater support. The vertical and horizontal stabilizers each have two main load bearing spars with ribs between them preserving

their shape. The rear spar is located at 35% chord from the trailing edge for the elevators and 37% chord for the rudders.

The two wing spars are located right behind the leading edge slats and right in front of the trailing edge flaps and ailerons. They are at 16% chord from the leading edge and 32% chord from the trailing edge respectively. The ribs are spaced at 20” apart with cutouts to allow fuel flow.

The remaining structure of the SB-01 is depicted below in Figures 8.3 and 8.4. The color-coating of the vehicle represent the materials described in Table 8.3.

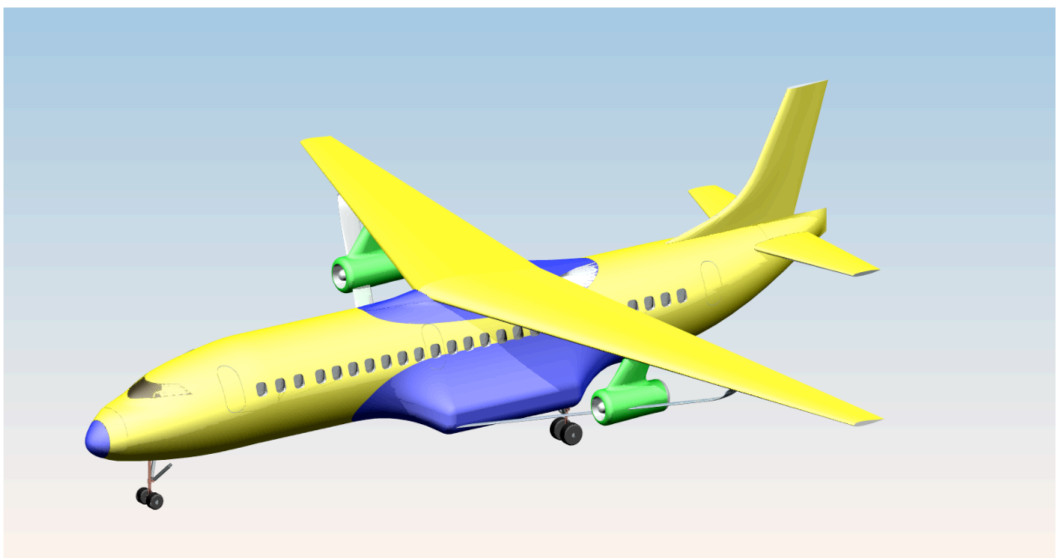

Figure 8.3 Exterior Material Representation of Aerohead SB-01

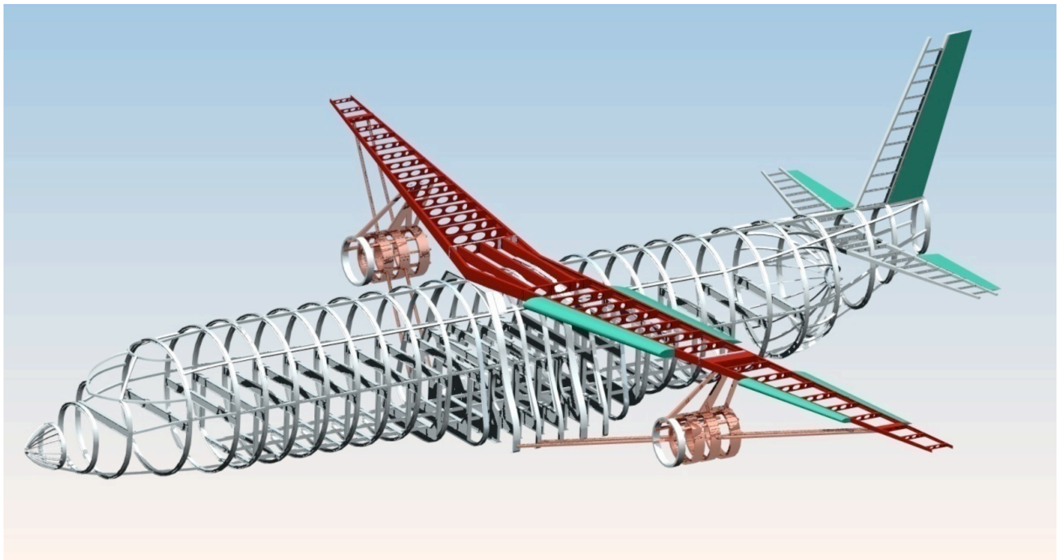

Figure 8.4 Material Representation of Aerohead SB-01with Control Surfaces Materials

Table 8.2 Color-code for Figures 8.3 and 8.4

Part	Material	Color
Wing Box	Carbon Fiber Reinforced Plastic	RED
Control Surfaces	Aluminum 2024-TO w/ GKN heating Mats	TEAL
Strut	Aluminum Alloy 7075-TO Titanium Alloy AMS 4914	COPPER
Engine Nacelle	Fiber-Metal-Laminate	GREEN
Skin	CFRP	YELLOW
Dome	Fiberglass	BLUE
Wing Transition	Fiberglass	BLUE
Landing Gear Pod	Fiberglass	BLUE
Bulkheads	Aluminum 2024-TO	SILVER

9. Stability and Control

Aerohead Aeronautics designed an aircraft that meets demands set by FAA, FAR, and the RFP. In doing so the SB-01 is comprised of traditional control surfaces and tail sizing to meet engine out flight conditions as well as a nose wheel lift off (nose up pitching moment). Various methods and programs were used in calculations for control surface sizing, neutral point calculation, and dynamic analysis. These analysis programs included *Tornado* Vortex Lattice Method (VLM) [26], *LDstab* (Lateral Directional Stability) [27] similar to DATCOM , and a VPI-NASA Excel spreadsheet. The *Tornado* program was used to find stability derivatives and the static margin which led to neutral point (NP) determination. *LDstab* (Lateral Directional Stability) [27] was also used to find stability derivatives and the proposed engine out criteria. VPI-NASA Excel spreadsheet provided numerous calculations for elevator, rudder, and aileron sizing as well as some dynamic analysis [46]. This program was designed by Virginia Tech. Aerohead Aeronautics evaluated the SB-01 at several conditions; for the engine out condition the aircraft was evaluated under take-off/sea-level parameters. To study the neutral point position, the aircraft was evaluated at cruise and maximum altitude. All control surfaces were properly sized for engine out flight condition, pitch control, roll rate and yaw effect. Flaps, slats and spoilers are also traditional additions to the SB-01 to produce maximum lift coefficients, and stability in roll and deceleration.

9.1 Vertical and Horizontal Tail Analysis

The vertical tail was sized so that the available yawing coefficient would exceed the required yawing coefficient in the instance of an engine out condition and for cross wind analysis. The vertical tail has a root chord of 10.33 feet, a tip chord of 6.58 feet and an overall area of 250.2 square feet. The vertical tail sits atop the fuselage and is 49.7 feet separated from the wing apex. This was done so that the SB-01 could achieve its best static margin percentage by moving the wing aft. The aspect ratio of the vertical tail is 1.36 and has the required area to fulfill engine out condition explained in more detail further in the report.

The horizontal tail was sized to meet the minimum static margin (of which was 14.89%) while maintaining the necessary ability for pitching moment on nose wheel lift-off. The horizontal tail is also located aft of the wing by 49.7 feet but sits below the wings vortex flow by 5.24 feet. This allows clean air to move across the horizontal tail and above the engines. It has an area of 386.3 square feet, a root chord of 11.25 feet, and a tip chord of 4.5 feet. The trim drag was found using methods from Roskam and Etkin and was found to have a C_{Dtrim} of 0.066. Figure 9.1 shows the stability of the low horizontal tail configuration compared to a high horizontal tail configuration. Aerohead Aeronautics wanted to integrate a low tail configuration to maintain stability at high angles of attack. At these high angles of attack, the SB-01 does not encounter instability due to the wake of the wing. In this case the SB-01 only has one trim point; On the contrary, a high horizontal tail configuration would have two trim points because the wake off of the wing interferes with the high tail configuration. If the second trim point is reached, the plane cannot recover. Thus, a stick shaker or angle of attack limiter must be implemented to prevent this condition [2].

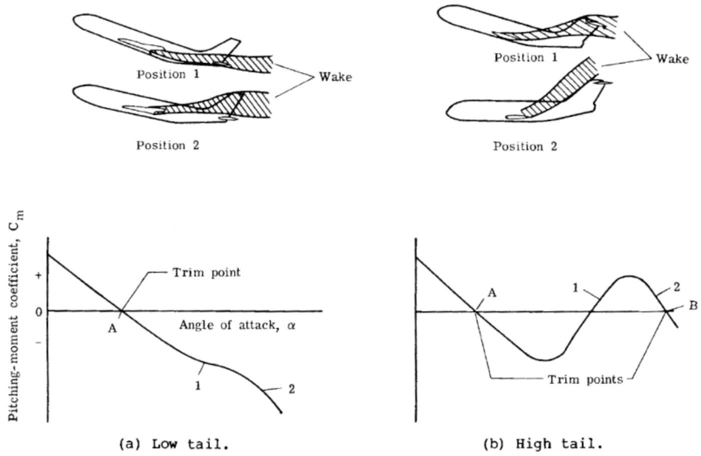

Figure 9.1 Relations of angle of attack to pitching moment coefficient [2]

Engine out analysis was done with the program *LDstab* [27] and was used on the basis that C_{Navail} is greater than $C_{Nrequired}$. This code was validated under the Boeing 747 parameters. The required yawing moment coefficient is the yawing coefficient required to maintain steady flight with one failed engine at $1.2V_{stall}$ which is required under FAR 25.149. The remaining engine will maintain maximum thrust of 20,000 lbs and the bank angle will not exceed 5°. Tornebeek's drag equation for the wind milling engine was used. Table 9.1 shows the variables found using *LDstab* and the coefficients comparatively.

Table 9.1 Engine out Analysis Parameters

Variable	Climb
β	1.856°
φ	5°
δ_a	2.82°
δ_r	20°
C_{navail}	0.0263
$C_{nrequired}$	0.00152

A small aileron deflection is necessary to keep the sideslip angle below 2° and important to keep the aircraft in steady flight. The rudder was sized to maintain crosswind and engine out

criteria; it is detailed in a later section. The rudder was sized to be the length of the vertical tail and 35% of the chord.

9.2 Neutral Point

Neutral point was found using *Tornado's* VLM [26], and modeled with 25 panels chord wise and 25 panels span wise across the main wing, horizontal stabilizer, and representation of fuselage. A model of the VLM can be seen in Figure 9.2. *Tornado* code was validated using a warren 12 planform wing and had a difference in calculation of one tenth of the static margin. Therefore the neutral point calculated is reasonable. The wing was moved forward to meet the best designed area for a static margin of 14.89% and a neutral point of 35.82 % of the MAC. This would allow the SB-01 to be very stable in flight. As fuel is used in flight the CG become closer to the NP and thus a 14.89% static margin ensures safety, and stability.

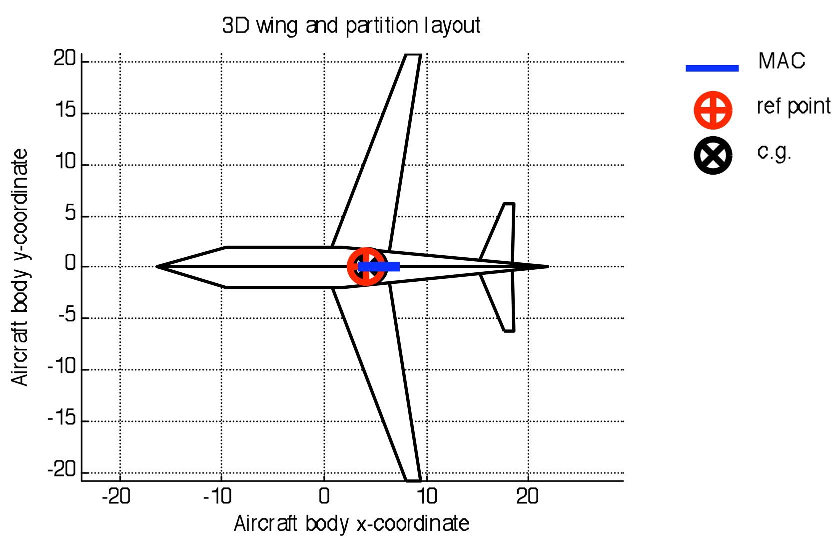

Figure 9.2 Tornado Vortex Lattice Method Output

9.3 Control Surface Sizing

The SB-01 is capable of completing all necessary in flight maneuvers. The following will detail the rudder, elevators, ailerons, flaps, slats and spoilers and the reasoning behind using them in flight. All control surfaces are NACA 0012 airfoils.

The rudder was sized to meet engine out flight criteria and was found to have an area of 52.76 square feet and is 35% of the chord of the vertical tail. The control surface is divided equally into two sections, to enable high speed yaw and low speed yaw. Only the bottom portion of the rudder is used during high speed flight, but at lower speeds the entire rudder is used. The top of the rudder is curved inward toward the tip of the nose of the aircraft. This shape with the aid of aerodynamic flow, permits the the tail rudder to move much easier. Figure on page 3 shows a detail drawing of this.

The elevators were sized appropriately to enable proper nose down pitching moment. The elevators span the horizontal tail with a length of 18.31 feet and have an area of 44.79 square feet. The elevators are able to lift the nose off the ground at a rate lower than calculated lift off speed from the BFL. Figure 9.3 shows the pitch angle in relation to the velocity needed to lift off the ground. The elevator is deflected at its maximum and the coefficient of moment and lift were used with the maximum pitch and flap controllers to achieve this sizing.

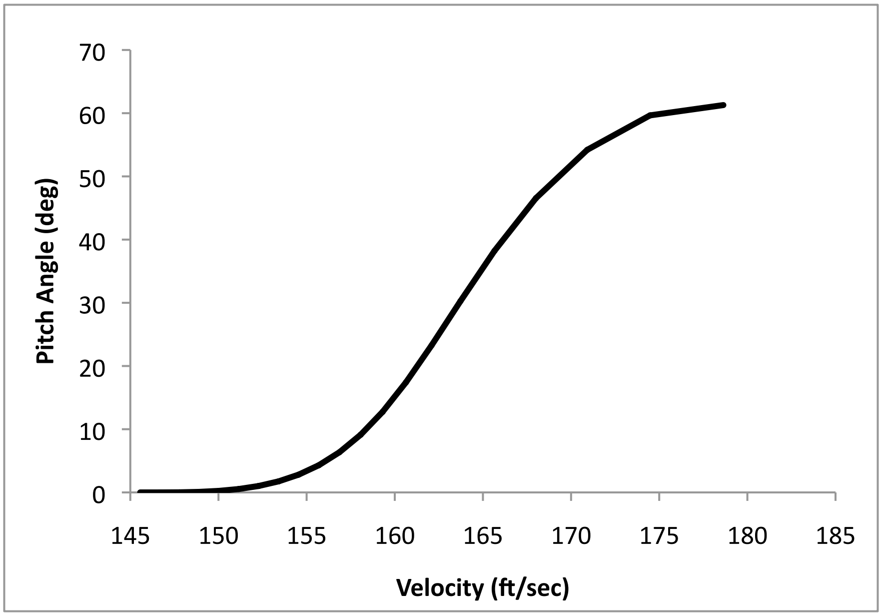

Figure 9.3 Velocity Required for Lift off with Sized Elevators vs. the Pitch Angle

Roll performance was evaluated so that the SB-01 would meet MIL-F 8785B roll performance specifications since FAA FAR regulations are so loosely defined. It states that for a class III aircraft that the plane must be able to roll 30° in 1.5 seconds. Figure 9.4 shows the time it takes for the SB-01 to roll in degrees. The Aerohead design meets the MIL standard and can roll 38° in 1.5 seconds. The ailerons were sized in accordance so that roll rate could be achieved but also so that during an engine out flight condition, with a maximum thrust of 20,000 lbs from the operable engine, the aircraft could trim appropriately. This was calculated using a stability three by three matrix involving the sums of all necessary stability derivatives. These can be seen in Tables 9.2 and 9.3. The required rudder and aileron deflections are 2.59° and 4.46°, respectively, to maintain steady flight for a sideslip angle of 3.88°. It was sized so that the ailerons would not have to deflect more than 20° and the rudder no more than 15°. Each aileron has an area of 67.43 square feet and is 20% of the chord. The following tables 9.2 and 9.3 display the six stability and control derivatives used to ensure stability for the aircraft.

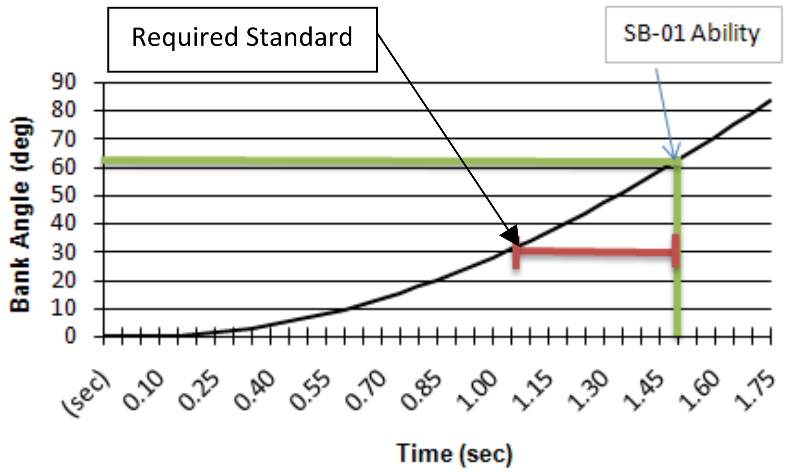

Figure 9.4 Roll Performance with Sized Ailerons vs. Time Required to Roll

Table 9.2 Control Derivatives of SB-01

Mission Station	**SB-01**
$C_{y\beta}$	-1.117
$C_{N\beta}$	-0.115
$C_{L\beta}$	-0.047
C_{Yr}	0.0096
C_{Nr}	0.0017
C_{Lr}	0.0043
C_{Lp}	-0.0516
C_{Np}	-0.0196
$C_{N\delta r}$	0.0812
C_{Mq}	-13.83
$C_{Y\delta r}$	-0.152
$C_{L\delta r}$	-0.009

Table 9.3 Stability Derivatives of SB-01

Mission Station	**SB-01**
Altitude (ft)	0
Mach	0.25
cg X direction (ft)	66.34
$C_{L\alpha}$	5.813
$C_{M\alpha}$	-0.865
S.M. %	14.89
N.P. MAC %	35.82

9.4 Dynamic Analysis and Flight Qualities

Methods from Etkin and Reid [20] were used with the derivatives found from *LDstab* stability code. The dynamic qualities were checked against the required values found in MIL-STD Class I Category B requirements. Category B includes non-terminal flight and is considered for climb cruise and descent. Table 9.4 shows Aerohead Aeronautics SB-01 dynamic analysis for longitudinal modes and lateral modes. The dutch roll mode is higher because at higher speeds the damping is larger. At a lower Mach number, it is expected that the dutch roll mode in damping to be lower due to the calculations of the stability derivatives being based upon the coefficient of lift. The short period and phugoid modes are within the correct range of allowable values. These two modes depend heavily on the speed of the aircraft which were tested to be at Mach 0.8. At these speeds the damping must be a little lower to keep the aircraft stable. Having positive pitch stiffness, (negative $C_{M\alpha}$) it allows the aircraft to be stable in static longitudinal flight. To maintain stability and control in flight, the use of a digital flight control system is employed to aid the pilot. This is further discussed in the Section 10.X, along with the remainder of the flight controls system.

Table 9.4 Dynamic Analysis of SB-01

		MIL-STD Cat. B Level 1 Requirements	SB-01
Short Period	Damping	0.3 < bξsp < 2.0	0.84
	Natural Frequency (rad/s)	0.8rad/s < ωsp < 2.0	1.72
Phugoid	Damping	ξPH > 0.04	0.838
Dutch Roll	Damping	ξPH > 0.19	0.32
	Natural Frequency	ωND > 0.4	1.7

10. Aircraft Systems

To compete with modern day aircraft, the Aerohead SB-01 design incorporates a wide variety of advanced technologies throughout all of the systems. Among these technologies are fly-by-light capabilities, large LCD panel displays, and bleedless de-icing systems.

10.1 Flight Control Systems

The primary flight controls are similar to those currently being installed on the Airbus A380, involving Goodrich electro-hydrostatic actuators (EHA). These control surface mechanisms are also equipped with electro-backup hydrostatic actuators (EBHA) as a failsafe. Goodrich systems are presently connected by fly-by-wire technology yet a switch to fly-by-light has been proposed. The advantages of EHAs are not limited to weight savings but also greatly reduce the maintenance required on the flight control systems.

The use of electricity to power these actuators eliminates the need for a heavy hydraulics system but still retains the power to deflect the control surfaces in order to efficiently maneuver

the aircraft. Two types of electro-hydrostatic actuators are needed for total control: linear and rotary. Linear actuators control the primary flight controls, specifically the deflection of ailerons, elevators, rudders, and spoilers. The ailerons and elevators are controlled by two linear hydrostatic actuators while the rudder is controlled by three and the spoiler by one. Additionally, Goodrich has developed a trimmable horizontal stabilizer actuator (THSA) that automatically moves the horizontal stabilizer to trim out and deflect the elevator as programmed by pilot or autopilot. This surface is powered by a single actuator using dual independently controlled electric motor drives.[28] Rotary actuators are used for secondary flight controls to extend and retract flaps and slats. The slat power control unit (PCU) includes an electric drive channel with a power-off brake as a failsafe. In the event that power to the PCU is lost, the slat transmission will be locked and provide additional braking, yet permits free-rotation while the solenoid is energized.

The EHAs installed on the SB-01, however, are controlled by fly-by-light technologies which have several advantages over the fly-by-wire. The utilized fiber-optic cables provide instantaneous response to flight commands due to the lack of electric motor delay caused by wire transmissions. Fiber-optic cables are also immune to electromagnetic interference that may be present from other operating electronic systems. By integrating this fast-response, power-by-wire system into the current control stick configurations used on the Boeing 737 and Airbus A320, the SB-01 flight control response will be far superior compared to the conventional hydraulics systems in use today.

10.2 Cockpit Systems

The SB-01 cockpit follows the configuration of existing commercial aircraft, specifically the Boeing 737-300, but relies on a variety of advanced navigation, communication, and display technologies. Honeywell Incorporated produces an array of integrated systems that are ideal for displaying and controlling multiple aspects of flight by a single piece of equipment, consolidating flight data, thrust and fuel management, as well as maintenance indicators to a single display.

The largest part of the SB-01 cockpit systems is the Honeywell Primus Epic Integrated Avionics System. Comprised of four 8-inch by 10-inch LCD displays as well as an additional 10-inch by 13-inch LCD in the center of the control console, the Primus Epic system provides multiple ways of displaying critical data. The software-based avionics provide a cost-effective solution for communication, navigation, and surveillance updates while allowing the pilot to customize the display to their individual preferences. The scalable displays permit charts, maps, and engine instrumentation to be resized for both two- and three-dimensional graphic models. The patented Graphical Flight Planning (GFP) and Integrated Navigation (INAV) is the first interactive navigation system that allows the simultaneous display of traffic, terrain, airspace, airways, airports, and navigation aids.[29]

The avionics also include the Honeywell Versatile Integrated Avionics (VIA) platform and a Rockwell Collins Autopilot computer. The Honeywell VIA has been certified on the Boeing 737NG for cycle-to-cycle concurrent monitoring. This single box also includes an ARINC 659 fail-passive communications path that guarantees the processing of flight critical functions. The Rockwell Collins Autopilot computer can be specifically programmed to meet the needs of the 2009 RFP and alleviate the workload of pilots throughout the commercial industry.[30] Additional weather, terrain, altitude, and navigation information are provided by Honeywell's high resolution multifunction radar display (MFRD) 6.24-inch by 4.82-inch display and the TRA 45A 3.26-inch square display. A complete display of the cockpit is shown in

Figure 10.1. Additional miscellaneous sensors and flight controls are provided by Honeywell and Rockwell Collins and are labeled below Figure 10.1.

To ensure familiarity for pilots that have flown Boeing 737s and Airbus A320s for the past decades, the cockpit is modeled in a similar fashion down to the control yokes. The landing gear, flap controls, autopilot, and other features are placed near their current locations in these existing aircraft so it takes only minutes for a pilot to become acquainted with the cockpit systems shown below.

Aerohead Aeronautics – SB-01

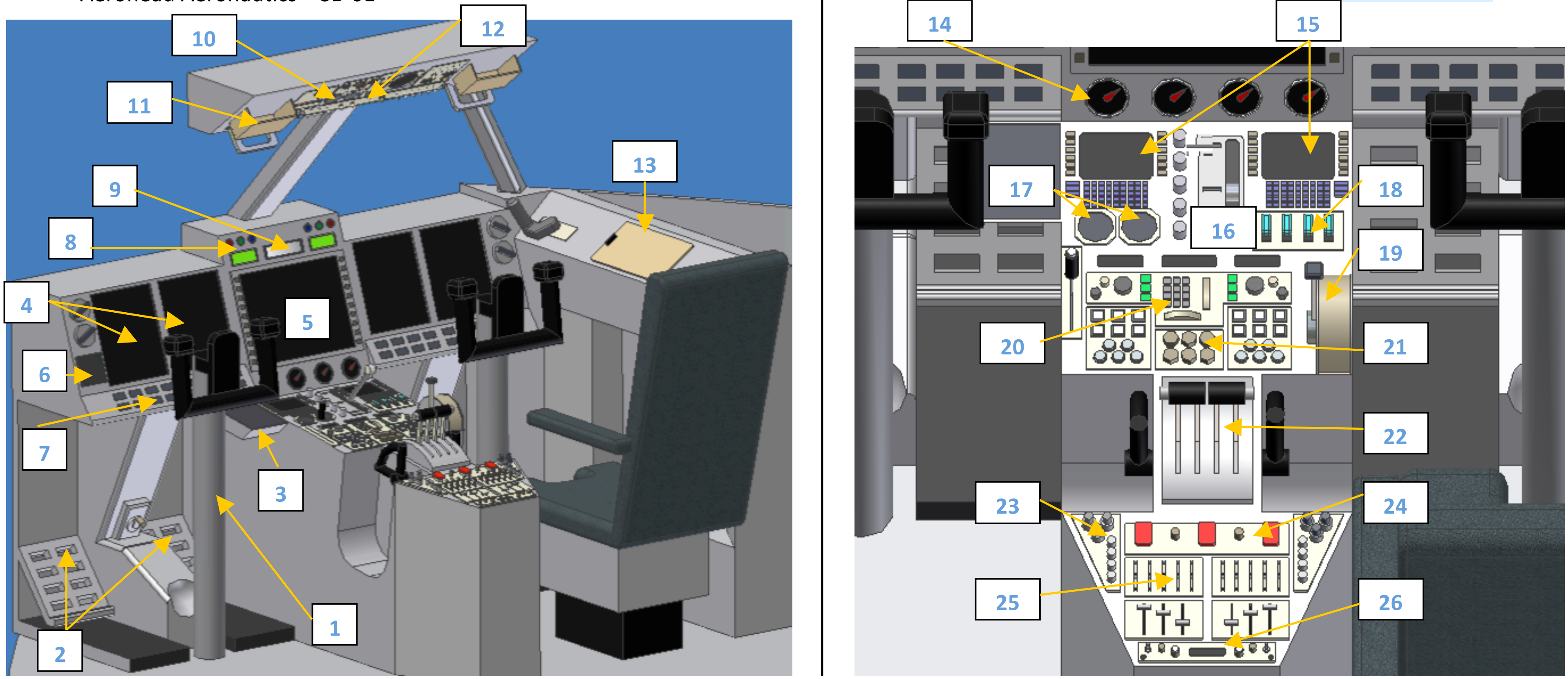

1	Control Stick	11	Chart Storage	21	Icing Controls
2	Control Pedals	12	Fuel Gauges	22	Throttle Controls
3	MFRD Screen	13	Clipboard	23	Misc. Controls
4	8” x 10” LCD Display	14	Altitude Indicators	24	Light Controls
5	10 x 13” LCD Display	15	Autopilot	25	Misc. Switches
6	TRA 45A Terrain Display	16	Landing Gear Controls	26	Radio Controls
7	Additional Display Controls	17	3.25” x 3.25” Displays		
8	Warning Lights	18	Lights		
9	Compass	19	Flap Controls		
10	Environmental Controls	20	Engine Start and Setup		

Figure 10.1 Aerohead SB-01 Cockpit

10.3 Electrical Systems

The electrical system of the SB-01 is vital to the flight control system so a series of back-up generators are required along with the standard APU and battery. A Honeywell 331-200A APU will provide the necessary power to start the twin PW1000G engines without the additional support from ground units. The 331-200A model is currently installed on the Boeing 757-200/300 as well as the 767-200/300/300F, which is a larger class of airliner yet meets the requirements set forth by the 2009 RFP. This APU fully meets all of the system needs in the case of an emergency up to altitudes of 35,000 feet and is certified to start and operate at flight levels up to 43,000 feet, which are the required cruise and cruise altitudes, respectively. This specific unit involves a two-stage axial turbine that increases engine life by initially requiring electrical power to start but then becomes a generator once it is operational, providing back-up electrical power in the event of a main engine power failure. The 331-200A APU operates at a lower volume due to the design of the inlet, compressor and hot section aiding in reducing the level of ground noise produced.[29]

For redundancy, a single lead acid battery is installed to provide utility DC power to start the APU and provide in-flight emergency power in the case the APU needs restarting. Two Honeywell 90 kVA generators are also installed and connected to a converter to provide the primary electrical power to the various aircraft systems during flight. A developing concept is also featured on the wings of the SB-01 that can generate a small amount of electrical power using wind energy. These wingtip turbines are currently being developed to generate enough energy to power small electrical systems, such as de-icers, and to alleviate trailing edge vortices produced by aircraft at takeoff.[31] The combination of these back-up systems assure that the electrically-based flight controls will remain operational for every flight condition.

10.4 Fuel System

The strut-braced airplane contains seven fuel tanks made of aluminum alloy. The main fuel tank is located between the front and rear spars at the 15% and 65% chord positions. Each wing contains 3 tanks that extend out to 78% of the span. The outer portion of the outboard wing tank does not contain any fuel. If needed, the fuel can be shifted inboard or outboard to provide inertial relief for the wing structure. Each wing fuel tank occupies 50% of the chord where the ratio of the volume of the integral wing tank to the externally measured volume is 0.85 (Figure 3.2). Table 10.1 contains the total fuel and volume for weight for both the wing and fuselage tanks.

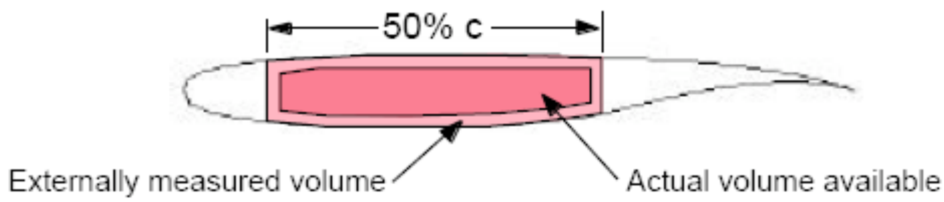

Figure 10.2 Cross-Section of Wing and Fuel Tank[32]

Table 10.1 Fuel Tank Sizing

	Total Fuel	**Wing Fuel**	**Compartment Fuel**
Fuel Weight (lbs)	33051	25974	7077
Fuel Volume (gal)	5110	4016	1094
Fuel Volume (ft^3)	683	537	146

10.5 Landing Gear

The SB-01 relies on a tricycle landing gear configuration to ensure that the aircraft can utilize existing loading technologies at current airports. The main gear consists of four wheels positioned aft of the center of gravity at 16º from the vertical. With this configuration, the nose landing gear carries seven percent of the static TOGW, which complies with Raymer[1], who proposes that the main gear carry approximately eighty-five to ninety-three percent of the total weight and the nose gear supports the rest. Following Raymer's guidelines, the SB-01 has a wheel track of 16.9 feet, producing a turn-over angle of 64º and a tail-strike angle of 18.5º.

Unlike conventional commercial airliners, the strut-braced wing is mounted on top of the fuselage making it difficult to integrate the landing gear into the wing-fuselage joint. However, to prevent a turn-over on takeoff or landing, the wheel track must be wider than the fuselage. To resolve this problem, the main gear retracts into two pods that are smoothly attached to the base of the fuselage. The SB-01 nose gear retracts aft into the fuselage while the main gear retracts forward, rather than tucking inward as the gear does on a Boeing 737. Figure 10.3 illustrates the gear in the stowed and active position.

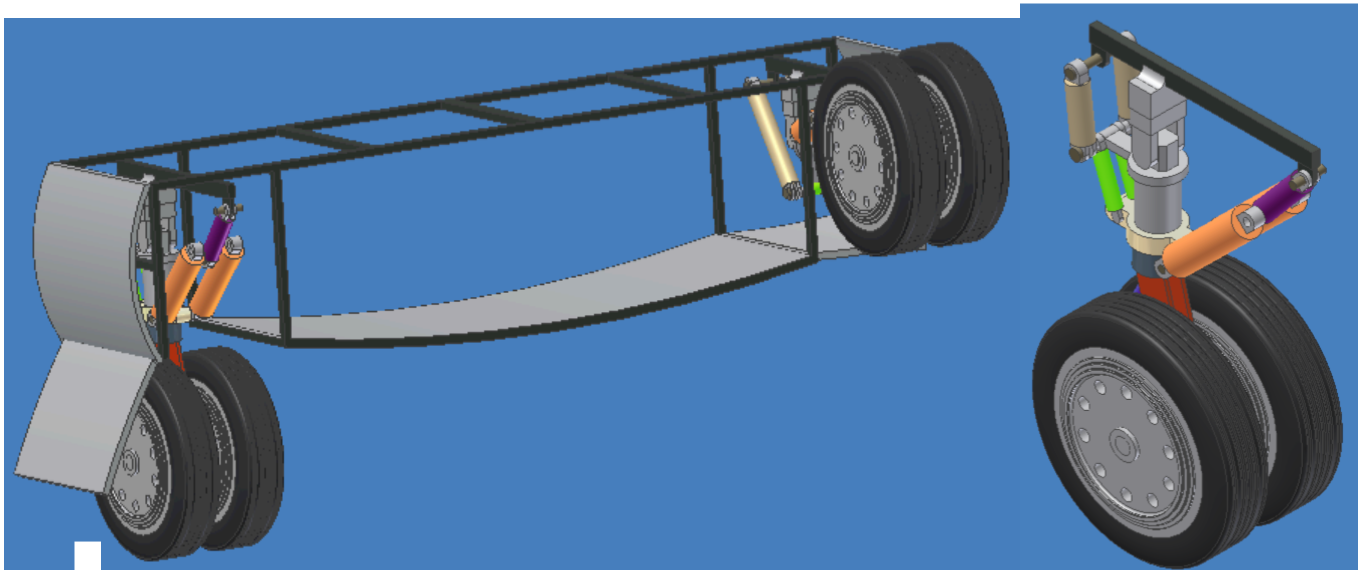

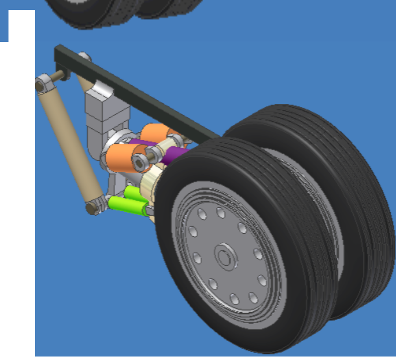

Figure 10.3 Aerohead SB-01 Landing Gear Assembly

The wheels are sized also according to Raymer's[1] guidelines and produced the following results. The main landing gear wheels are 42-inches in diameter and 14.75-inches wide. The nose gear consists of two wheels of 23.1-inches diameter and 5.95-inches wide. Michelin's new AIR X radial tires offer 20-30% weight savings over bias-ply tires and have proven to increase tread life by up to 50%. These tires also have increased overload capacity as well as resistance to cuts causing a reduction in maintenance and life cycle costs.[33]

10.6 Lighting System

The Aerohead SB-01 features the Honeywell Astreon series of high performance exterior lighting which is federally mandated by the FAA. These LEDs are much more reliable than the typical halogen bulbs and have an extended lifespan. The endurance of these lights lowers labor costs for bulb replacement or repairs and allow for the maintenance or inspection of any element to be performed at night.[29] The lighting system is configured as displayed below in Figure 10.4.

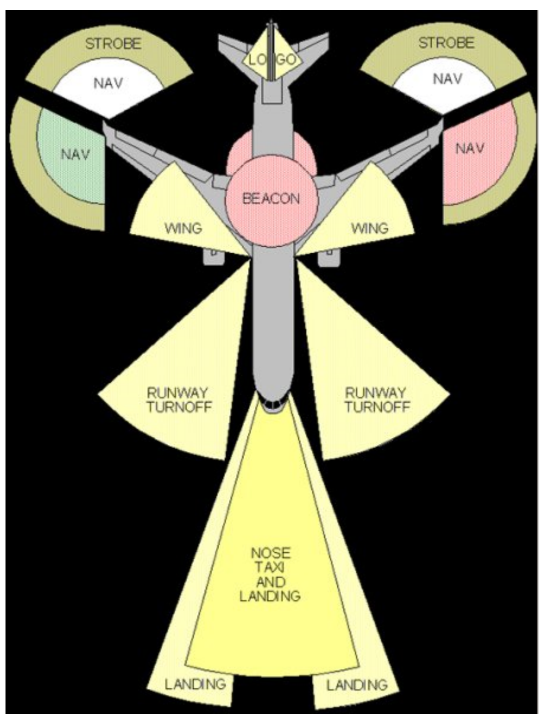

Figure 10.4 Exterior light configuration for Aerohead SB-01 Design[34]

10.7 Anti-Icing System

Although bleed air will be utilized for interior cooling and oxygen, it will not be used for de-icing the control surfaces of the wing. An anti-icing fluid will be sprayed on the wing surfaces prior to take-off but the SB-01 incorporates a new heating system designed by GKN Aerospace. The newly developed system that is currently being installed on the Boeing 787 *Dreamliner* consists of several heating mats formed through multiple layers of composites. A base layer of carbon fiber is woven and then covered with a layer of dry woven glass fabric to provide insulation between the carbon fiber and the metal spray. The metal is then sprayed on using a hand sprayer and cooled to solidify before the necessary electronic wiring is attached. The metal is then covered with another layer of glass fibers and a final layer of carbon fiber prior to being shaped and formed to fit the slat and flap surfaces. These systems require minimal electricity and feature elaborate wiring that allow for the full maneuverability of the slat. The mats, shown in Figure 10.5, operate at temperatures between 45º and 70º F in order to break the adhesion of the ice to the surface.[35] Goodrich sensors are used to automatically initialize de-icing during flight yet also alert the crew for manual de-icing control. The absence of bleed air being blown through the surfaces greatly reduces the noise emissions of the de-icing process assisting in the overall noise reduction of the aircraft.

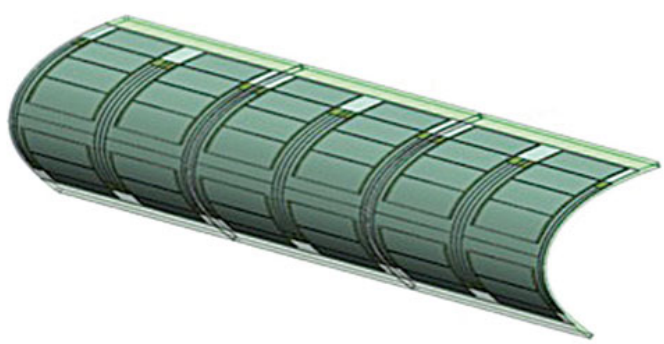

Figure 10.5 Anti-icing heating mat by GKN Aerospace that attached to the control surfaces of the SB-01 wing[35]

10.8 Environmental Control Systems

The cabin of the SB-01 features newly developed systems from both Donaldson and Goodrich for air quality and control. Air is bled from the engine inlets into a Donaldson bleed air filter and then proceeds to an air purification system (APS). The air is then cooled and ran through a series of Donaldson BIOAdvantage antimicrobial filters and circulators prior to being pumped into the cabin. The BIOAdvantage system captures and neutralizes microorganisms within the air, producing clean air for passengers and crew. Additional filters are used for humidification, odor removal, electronics cooling, and high-temperature air flow.[36]

The galley of the SB-01, displayed in Figure 10.6, is designed by JAMCO. The galley features two programmable microwaves, an A818-1 air chiller, and nine removable storage containers for miscellaneous blankets, pillows, or food items. There are three service cart bays with locks to restrain the carts while not in use as well as several lockable cabinets for additional storage space. The cockpit door is intrusion resistant as well as ballistic-proof. It is secured by three latches: one pressure latch, an electronic latch, and a standard mechanical latch that are all regulated by a keypad lock. The galley wall also features foldable seats that permit the crew to move freely throughout the galley while in flight.

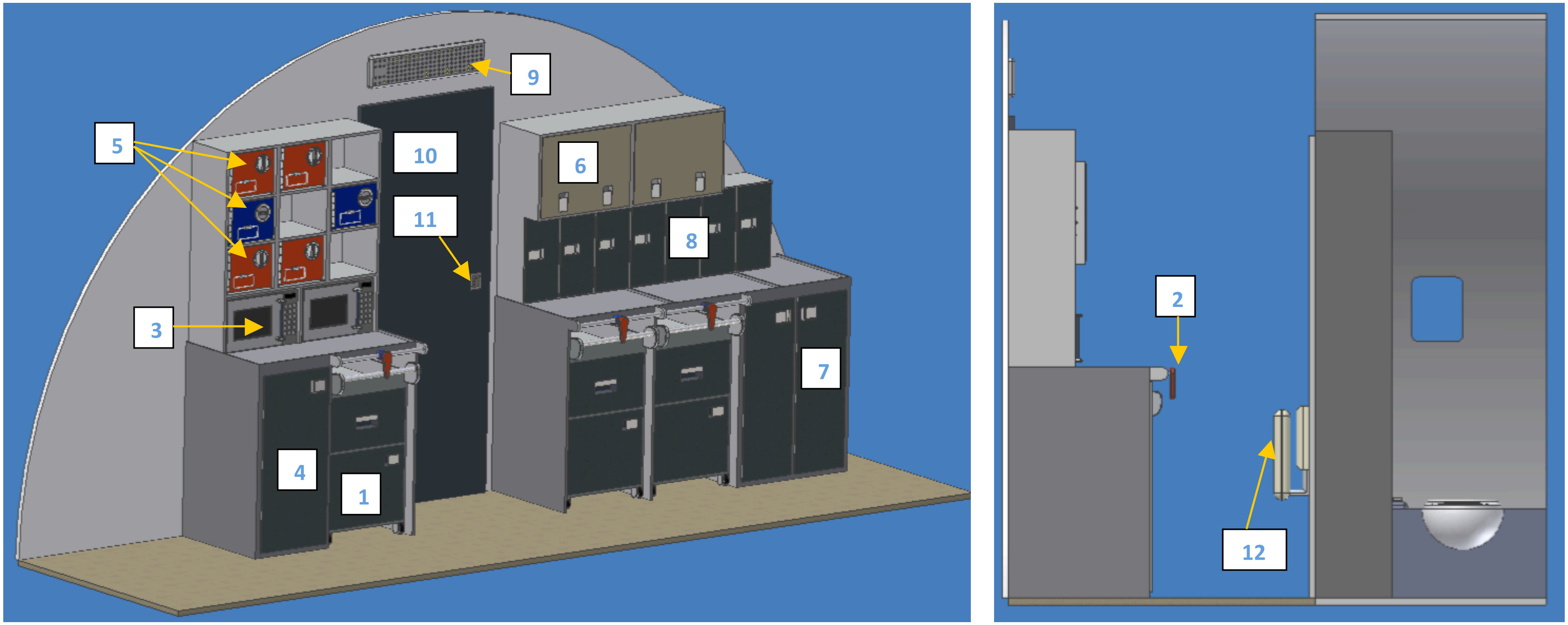

1	Service Cart	7	Food Storage
2	Cart Lock	8	Miscellaneous Cabinets
3	Microwave	9	Cabin Seat Indicators
4	A818-1 Air Chiller	10	Cockpit Door
5	Removable Storage Container	11	Keypad Lock
6	Blanket and Pillow Storage	12	Foldable Crew Seat

Figure 10.6 Aerohead SB-01 Galley display

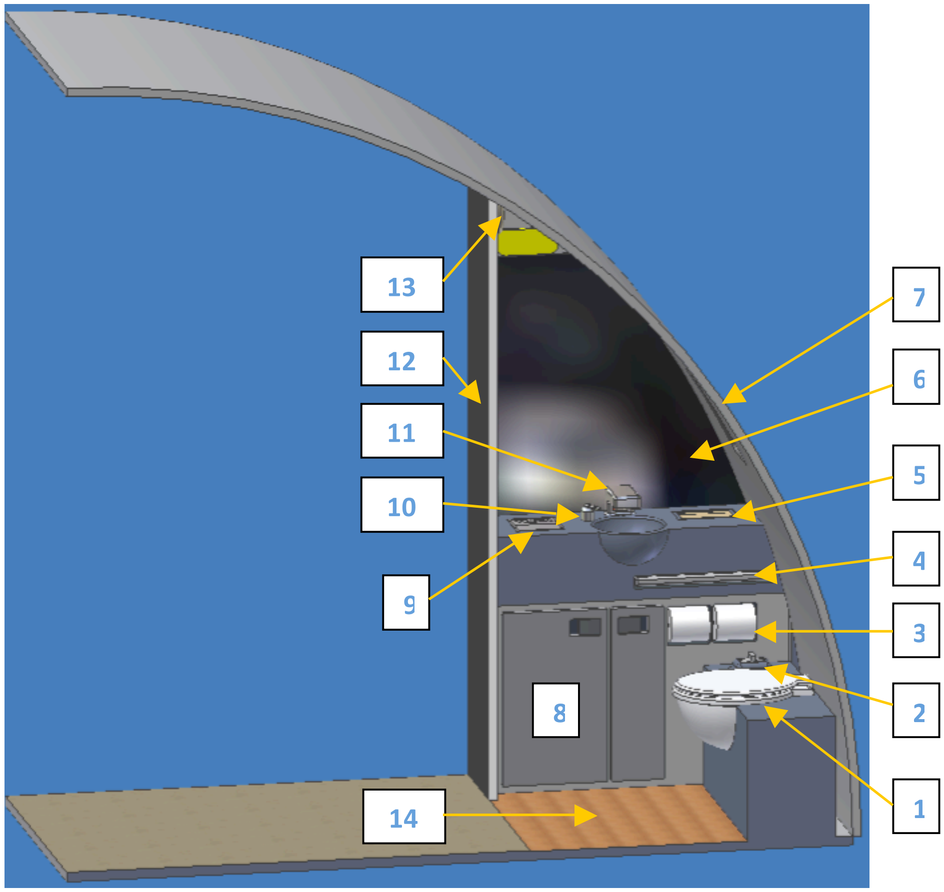

1	Toilet	8	Storage
2	Flush Lever	9	Trash Can
3	Toilet Paper Rack	10	Infrared Soap Dispenser
4	Extendable Changing Table	11	Infrared Faucet
5	Paper Towel Dispenser	12	Light/Fan Control
6	Half-wall Mirror	13	Smoke Detector
7	One-touch Window	14	Composite Hardwood Floor

Figure 10.7 Aerohead SB-01 Lavatory

The lavatory is also designed by JAMCO and can be seen in Figure 10.7. It features an infrared, wall-mounted faucet as well as an infrared soap dispenser. Water is supplied and heated by a Goodrich corrosion resistant heater and potable water controller, complete with heated drain masts that assure continuous water flow. A JAMCO PU 90-101 smoke detector is installed on the lavatory wall as well as throughout the cabin, featuring six heat and smoke detecting sensors.[37] The lavatory is complete with a half-wall mirror, a granite-looking composite counter, a liquid crystal window that changes from translucent to opaque at the touch of a button, and an extendable changing table. Cabinets are also located under the sink for bathroom necessities and storage.

10.9 Cargo Loading System

The luggage aboard this aircraft will be stored in two main locations, the overhead compartments in the main cabin and below deck. To meet the RFP, each passenger will have at least 7.5 cubic feet which is a total of 1125 cubic feet of luggage space on the aircraft. The overhead compartments will have a total of 666 cubic feet of luggage space. This is not always organized properly when used or even used that much, which means a lot of that is wasted space. This means that there still needs to be more than enough space below deck to hold the required luggage.

The luggage below deck will be held in LD2 containers, each container can hold up to 120 cubic feet of space, shown in Figure 10.8.

Figure 10.8 LD2 Container[38]

The LD2 containers below deck will be place in rows of two to minimize the wasted space below deck. To make sure that there is enough storage space below deck for all the luggage, Table 10.2 has been created to examine three different configurations. Each different configuration has a different number of LD2 containers.

Table 10.2 Configuration of Luggage Containers Below Deck

# of LD2 Containers	Length of Luggage Compartment (ft)	Total Luggage Volume (ft^3)	Volume of Luggage per Passenger (ft^3)
4	10.1	1146.2	7.6
6	15.1	1386.2	9.2
8	20.1	1626.2	10.8

As seen in Table 10.2, four LD2 containers will successfully pass the requirement set by the RFP, but with all the wasted in the overhead compartments there will not be enough room. The case with eight LD2 containers is chosen for the SB-01 design. This will provide sufficient luggage space below deck and the volume per passenger is well above the requirement of the RFP.[35]

11. Cost

The RFP requires the design of a commercial transport aircraft whose acquisition cost is similar to other comparably sized commercial transports in typical U.S. airline operation. The primary focus includes an 8% reduction in total operating cost per available seat mile with a design objective of 10% or better. Assuming a fuel cost of $2.50/US gal, the competition also requests an estimate for both flyaway and life cycle costs for a production run of 500 and 1500 units. Aerohead Aeronautics uses existing cost estimating methods for an initial analysis and optimizes each cost by incorporating current technologies.

11.1 Life Cycle Cost

The life cycle cost of an airplane program (LCC) includes the costs of research, development, testing and evaluation (RDTE), acquisition, operation and support, and the disposal of the airplane. The disposal of the airplane accounts for 10% of the total LCC. Equations used in the cost analysis were taken from Roskam's cost estimating method. All of the equations were functions of the airplane's empty weight, maximum velocity, technology factors, and the costs of the avionics systems and engines.

11.2 Research, Development, Testing, and Evaluation

The RDTE phase covers the planning and conceptual design, preliminary design and system integration, and the detailed design and development. Table 1 shows the various dollar rates used during the RDTE phase of the program. The man hours spent on airframe engineering and design, tooling, and manufacturing equaled 267.609 million hours. An RDTE production rate of 0.33 units per month was used with a manufacturing rate of 26 units per month. 4 airplanes were produced for the RDTE phase, which included 2 flight test airplanes and 2 airplanes for static testing that were not equipped with engines or avionic systems. The cost of avionics per RDTE airplane made up 15% of the airplane market price. The number of airplanes produced to production standard includes the two production runs of 500 and 1500 units and the 4 airplanes built during the RDTE phase. The cost to finance the RDTE phase equaled 10% of the total RDTE cost.

Table 11.1 Current Research, Development, Testing and Evaluation Rates

RDTE	Rate USD/hr
Engineering Dollar	104.811
Manufacturing Dollar	58.41924
Tooling Labor Dollar	75.60137

11.3 Acquisition

The total acquisition cost associated with the airplane program was a function of the number of airplanes produced to production standard, the number of airplanes produced during the airplane program, total manufacturing cost and the profit made by the manufacturer. The cost to finance the manufacturing phase made up 10% of the total manufacturing cost. Another 10% of the total manufacturing cost went towards profit. The total acquisition cost was found by subtracting the profit from the total manufacturing cost. Table 2 shows that the acquisition cost increased as the number of aircraft increased. Increasing the production quantity causes the engineering, tooling, manufacturing, and quality and control costs to increase. The strut-braced wing has the lowest total acquisition cost due to the aircraft's low take-off gross weight. However, the strut-braced wing still remains close to the comparative aircraft in total acquisition cost.

Table 11.2 Total Acquisition Cost Comparison [39]

Aircraft Type	500 Units $USD Billions	1500 Units $USD Billions
Strut-Braced	20.43	48.25
737-700	22.13	51.75
A320-200	24.19	57.00

11.4 Program Operating Cost

The operating costs were divided into direct and indirect operating costs. Direct operating costs (DOC) refer to the flying costs as a result of utilization of the aircraft. Indirect operating costs (IOC) arise as a result of operating commercial airline services. Equations 11.1 and 11.2 were used to estimate the airplane program's direct and indirect operating costs

$$C_{ops_{dir}} = (DOC) * (R_{bl_{ann}}) * (N_{yr}) \tag{11.1}$$

$$C_{ops_{dir}} = (IOC) * (R_{bl_{ann}}) * (N_{yr}) \tag{11.2}$$

where $R_{bl_{ann}}$ denotes the total annual block miles flown and N_{yr} represents the number of years during which the airplane is operated. $R_{bl_{ann}}$ is expressed in nautical miles per airplane and is dependent on block speed and annual utilization.[40] Table 11.3 shows the quantities required to estimate the DOC, which is expressed in U.S. dollars per available seat mile (ASM). Figure 11.1 provides an overview of the direct operating cost using the data located in Table 11.3.

Table 11.3 Direct Operating Cost of SB-01

Variables	Value
Block Distance (nm)	2800
Block Time (hrs/trip)	7.08075
Block Speed (nm/h)	420.16253
Serviceable Operating Days (days/year)	365
Usable Hours per Day	14
Flight Frequency (rips/day)	1.97719
Annual Utilization (hrs/yr)	5110

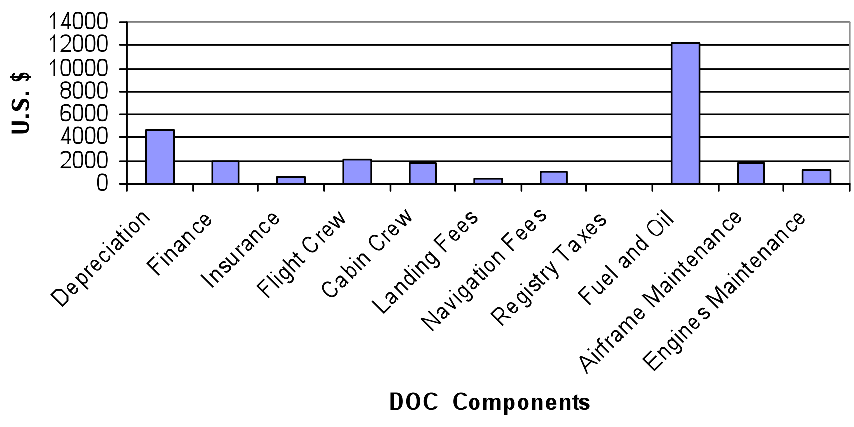

Figure 11.1 Direct Operating Cost Breakdowns

The costs were analyzed over a depreciation period of 20 years with a residual of 10%. Figure 11.1 indicates the strong effect of fuel price on the direct operating cost, making up

44.184% of the total DOC.[41] The results show a total direct operating cost of $27,910.107 per trip with a cost per available seat-mile of $0.06645. The indirect operating cost was an estimated 50% of the DOC, which resulted in a total operating cost of $41,865.160 per trip. This produced a total operating cost per available seat mile of $0.09968 for a 2800 nm mission range.

Table 11.4 Passenger Airline Systems (Cents per Available Seat Mile)[42]

Airline Group	3rd Quarter 2007	4th Quarter 2007	1st Quarter 2008
Network	13.6	14.5	15.3
Low-Cost	9.6	9.5	10
Regional	14.7	14.9	16.3
21-Carrier Total	**12.8**	**13.6**	**14.4**

Table 11.4 contains airline financial data from the Bureau of Transportation Statistics. The data was collected while jet fuel was $2.50 per gallon, resulting in an average operating cost per ASM of $0.136. The strut-braced wing shows a 26.71% reduction in operating cost per ASM in relation to other comparably sized commercial transports in typical U.S. airline operation. This exceeds the RFP requirement by 16.71%.

Table 11.5 Total Life Cycle Cost for SB-01

Life Cycle Cost	500 Units USD Billions	1500 Units USD Billions
RDTE Total	3.77	3.77
Acquisition Total	20.43	48.25
Program Operating Cost Total	213.29	639.88
Disposal Total	26.39	76.88
Total	263.89	768.78

Table 11.5 shows the total life cycle cost and the sum of each of the individual costs that make up the LCC. The results show an increase in LCC as the number of aircraft produced increases due to interest and depreciation costs. The operating cost is much larger than the

acquisition cost and the RDTE cost is much smaller than the acquisition cost, giving the following inequality:

$$C_{OPS} > C_{ACQ} > C_{RDTE} \tag{11.3}$$

Excluding the number of years operated by the customer, Table 5 indicates that the conceptual and preliminary design phases (part of the RDTE) are responsible for most of the life cycle cost of an airplane. Increasing the RDTE costs would ultimately lower the LCC for the customer.

11.5 Flyaway Costs

The Roskam Costing Method was used to estimate the flyaway costs of the Boeing 737-700, Airbus A320-200, and the strut-braced wing. Both recurring and nonrecurring costs were considered in the total flyaway cost estimation. Recurring costs included the airframe, engines and avionics. The nonrecurring cost analysis focused on the number of hours required for research, development, testing and evaluation. The production by the engineering, tooling, manufacturing, and quality control groups was also a factor in the nonrecurring cost estimation.

Table 11.6 Total Flyaway Cost Comparison for SB-01

Aircraft Type:	**500 Units USD Billions**	**1500 Units USD Billions**
Strut-Braced	28.48	61.21
737-700	31.04	65.89
A320-200	36.82	78.89

Table 11.6 shows that the total flyaway cost decreases as the fleet size increases. Flyaway costs rely heavily on aircraft take-off weight, which gives the strut-braced wing a slight advantage. Table 11.7 gives the aircraft delivery price, which was found by dividing the total flyaway cost by the number of aircraft units.

Table 11.7 Aircraft Delivery Price Comparison

Aircraft Type	500 Units USD Millions	1500 Units USD Millions
Strut-Braced	56.96	40.81
737-700	62.08	43.92
A320-200	73.65	52.59

According to Jane's 2008-2009, the aircraft estimated price (AEP) range of a Boeing 737-700 falls between 57 and 67.5 million dollars. The AEP for the Airbus A320 series ranges from 73.2 to 80.6 million dollars. The data for both comparative aircraft agrees well with existing data, which means that the cost estimations for the strut-braced wing are relatively accurate. Table 7 shows a 5.11807 million dollar reduction in AEP from the 737-700 and a 16.68622 million dollar reduction from the A320-200. Avionics were assumed to make up 22% of the A320's AEP due to Airbus's traditionally expensive avionics hardware platforms. This explains the large price gap between the A320-200 and the strut-braced wing.

12. Conclusion

Aerohead Aeronautics began designing the SB-01 by comparing similar 150 seat commercial airlines currently in service; this lead to three initial designs, the cantilever wing, blended wing body and strut-braced wing. After comparing these designs, the strut-braced wing was chosen for our final design. This design was then sized to the specifications set in the RFP, determining the overall length, due to the 150 person capacity and 7.5 cubic feet per passenger cargo capacity; thrust, due to the Mach 0.78 cruise speed and 43,000 foot maximum operating altitude; and lift, due to the 135 knot maximum landing speed and 7000 foot maximum takeoff field length.

The SB-01 uses a combination of new engine, wing, and materials technology to satisfy the RFP requirements. The SB-01 holds 150 passengers with a dual seating configuration and 168 passengers in a high capacity configuration. Combining overhead compartments and LD2 containers in a cargo hold the cargo capacity exceeds the 7.5 cubic feet per passenger requirement with 10.8 cubic feet of luggage per passenger. The plane's maximum range is 3024 nm instead of the RFP's requirement of 2800 nm. With the thrust of two PW1000G and a wing designed with a drag divergence Mach number of 0.84 the SB-01 meets the objective Mach number of 0.8 for long range cruise. The wing and engines also allow the plane to achieve an absolute ceiling altitude of 43,500 feet. The wing also allows a landing speed of 130 knots which is below the RFP requirement of 135 knots. The take off field length is well below the 7000 foot requirement with a distance of 4948 feet. The noise produced from this plane fulfills the RFP requirement by reducing the noise level 26 decibels below ICAO Chapter 4. The operating cost well exceeds the objective reduction of 10% by having a total reduction of 26.7%. The SB-01 will be certifiable to appropriate FARs for entry into service by 2018. Overall the SB-01 meets and in most cases surpasses all of the requirements provided by the AIAA RFP.

13. References

[1]Raymer, Daniel P. *Aircraft Design: A Conceptual* Approach. 4th ed. Reston, VA: American Institute of Aeronautics and Astronautics, 2006.

[2] “Subsonic Aircraft: Evolution and the Matching of Size to Performance” 8 Dec 2008 <http://www.ultraligero.net/Cursos/varios/aviones_subsonicos.pdf>.

[3] “Civil Turbojet/Turbofan Specifications.” 5 Dec 2008 <http://www.jet-engine.net/civtfspec.html>

[4] Hepperle, Martin. “JavaFoil.” 27 Jan 2007. Martin Hepperle. 20 March 2009. <http://www.mh-aerotools.de/airfoils/javafoil.htm>.

[5] “The GE90-An Introduction.” 18 Nov 2008 <http://www.anirudh.net/seminar/ge90.pdf>.

[6] “Better Vibrations for Turboprop Technology.” International Beat. American Institute of Aeronautics and Astronautics. 18 Nov 2008 <http://www.aiaa.org/aerospace/images/articleimages/pdf/International%20Beat1.pdf>.

[7] “Driving GE Ecomagination with the Low-Emission GEnx Jet Engine.” 20 July 2005. GE Aviation. 20 Nov 2008 < http://www.geae.com/aboutgeae/presscenter/ genx/genx_20050720.html>.

[8] “Preparing for the Future of Aircraft Engines - TECH56.” Aerospace Engineering and Manufacturing Online. SAE International. 16 Oct 2008 <http://www.sae.org/aeromag/features/aircraftengines/01.htm>.

[9] “CFM56-7B Turbofan Engine.” CFM: The Power of Flight. 12 Nov 2008 <http://www.cfm56.com/index.php?level2=products&level3=cfm56-7b>.

[10] Donoghue, J.A. “Cool Burnings.” ATW. 18 Nov 2008 <http://www.atwonline.com/magazine/article.html? articleID=1546>.

[11] “Pure Power PW 1000G.” Pratt & Whitney. 12 Nov 2008 <http://www.pw.utc.com/vgn-ext-templating/v/index.jsp?vgnextoid=59ab4d845c37a110VgnVCM100000c45a529fRCRD.

[12] Walsh, Joe. “Advanced Open Rotor Aircraft Workshop.” Rolls Royce. 18 Nov 2008 <http://www.omega.mmu.ac.uk/Open-Rotor-Workshop-24-June/An%20Industry%20Perspective%20Joe%20WalshRolls%20Royce.pdf >.

[13] “Nicolai's sizing program” 10 November 2008 < http://www.aoe.vt.edu/~mason /Mason_f/MRsoft.html#Nicolai>

[14] “737-700 Technical Characteristics” 12 November 2008 < http://www.boeing.com/ commercial/ 737family/pf/pf_700tech.html>

[15] “Aircraft Famlies/A320 Specifications” 12 November 2008 < http://www.airbus.com /en/ aircraftfamilies/a320/a320/specifications.html>

[16] Roskam, Dr. Jan. “Part V: Component Weight Estimation.” Airplane Design. Lawrence, Kansas: DARcorporation, 2003. 67-125.

[17] Roskam, Dr. Jan. “Part VII: Determination of Stability, Control and Performance Characteristics: FAR and Military Requirements.” Airplane Design. Lawrence, Kansas: DARcorporation, 2003.

[18] "Aircraft Data and History." Airliners.net. 3 Sep. 2008<www.airliners.net>.

[19] Smith, M. “Modeling Landing gear noise with installation effects.” American Institute of Aeronautics and Astronautics 13th Aeroacoustics Conference. 21 May 2007.

[20] Dobrzynski, W. “Research into Landing Gear Airframe Noise Reduction.” American Institute of Aeronautics and Astronautics 8^{th} Aeroacoustics Conference. 17 June 2002. Breckenridge, Colorado.
[21] Etkin, Bernard; Reid, Lloyd. Dynamics of Flight Stability and Control third edition. University of Toronto. John Wiley & Sons, INC. 1996.
[22] "Carbon fiber reinforced plastic." *Wikipedia, The Free Encyclopedia*. 21 Nov 2008, 19:07 UTC. 25 Nov 2008 <http://en.wikipedia.org/w/index.php?title=Carbon_fiber_reinforced_plastic&oldid=253242219>.
[23] *CES EduPack Selector Version 4.8.0*. CD-ROM. Granta Design Limited, 2008.
[24] "MHI Ships First Composite-Material Wing Box for the Boeing 787.” Mitsubishi Heavy Industries LTD News. 14 May 2007. 2 April 2009 <http://www.mhi.co.jp/en/news/story/200705141172.html>.
[25] "GLARE (material)." *Wikipedia, The Free Encyclopedia*. 22 Feb 2009, 20:30 UTC. 15 Apr 2009 <http://en.wikipedia.org/w/index.php?title=GLARE_(material)&oldid=272566273>.
[26] “Tornado VLM.” 20 February 2009 < http://www.aoe.vt.edu/~mason/Mason_f/ MRsoft.html#Nicolai>.
[27] “LDstab sizing program.” 20 February 2009 < http://www.aoe.vt.edu/~mason /Mason_f/MRsoft.html#Nicolai>.
[28] “Actuating and Landing Systems.” Goodrich Corporation. 4 March 2009 <http://www.goodrich.com/portal/site/grcom/home>.
[29] "Honeywell Air Transport and Regional". Honeywell International Incorporated. 20 March 2009 <https://commerce.honeywell.com/webapp/wcs/stores/servlet/eHomePage?storeId=10651>.
[30] "Avionics Systems Catalog". Rockwell Collins Incorporated. 20 March 2009 <http://www.rockwellcollins.com/products/cs/at/avionics-systems/index.html>.
[31] Patterson, James C. “Wingtip Vortex Turbine.” U.S. Patent 4,917,332. 17 Apr, 1990. <http://www.aoe.vt.edu/research/groups/tbw/reports/mad/sbw_mad_center98.ppt>.
[32] "Air X Radial Tires". Michelin Aircraft Tire Company. 4 April 2009 <http://www.airmichelin.com/commercial.html>.
[33] Yoon, Joseph. "Aircraft Lighting.” AerospaceWeb.org. 13 March 2009 <http://www.aerospaceweb.org/question/electronics/q0263.shtml>
[34] Sloan, Jeff. "High Performance Composites". Composites World. 18 February 2009 <http://www.compositesworld.com/articles/787-integrates-new-composite-wing-deicing-system.aspx>.
[35] “Filtration Solutions.” Donaldson Company. 22 March 2009. <http://www.donaldson.com/en/index.html>.
[36] “Aircraft Interiors.” JAMCO Corporation. 22 March 2009 <http://www.jamco.co.jp/e/index.html>.
[37] Grasmeyer, Joel M. “Multidisciplinary Design Optimization of a Strut-Braced Wing Aircraft.” 13 April 1998. Aerospace and Ocean Engineering Department, Virginia Tech. Blacksburg, VA. 16 March 2009 <http://scholar.lib.vt.edu/theses/available/etd-4598-173228/unrestricted/Thesis.pdf>.

[38] "Nordisk Containers." Hydro Nordisk Aviation Products. 13 April 2009. <http://www4.hydro.com/nordisk/library/ images/products/nordisk_containers/half_width_containers/ake_ld3/ld3.jpg>.

[39] Fraes, Paul. Jane's All the World's Aircraft 2008-2009. Alexandria, Virginia: Cambridge University Press, 2008.

[40] Roskam, Dr. Jan. "Part VIII: Airplane Cost Estimation: Design, Development, Manufacturing and Operating." Airplane Design. Ottawa, Kansas: DARcorporation, 2003.

[41] Horder, Peter. "Airline Operating Cost." SH&E International Air Transport Consultancy. 22 Jan 2003. United States Department of Transportation. 15 March 2009 <http://www.soton.ac.uk/~jps7/Aircraft%20Design%20Resources/Cost%20data/Airline %20operating%20costs.pdf>.

[42] Smallen, Dave. "3rd Quarter 2008 System Airline Financial Data." Bureau of Transportation Statistics. 15 Dec 2008. United States Department of Transportation. 15 March 2009 <http://www.bts.gov/press_releases/2008/bts061_08/html/bts061_08.html>.

[43] Bertin, John J. *Aerodynamics for Engineers*. 4th ed. Saddle River, NJ: Pearson Education, 2002.

[44] Anderson, John D. *Introduction to Flight*. 5th ed. New York, NY: McGraw Hill Higher Education, 2005.

[45] Laurence K. Loftin, Jr., "Subsonic Aircraft: Evolution and Matching of Size to Performance," NASA RP 1060, August 1980.

[46] "VPI-NASA" Excel sizing spreadsheet." 02 March 2009 < http://www.aoe.vt.edu/~mason /Mason_f/MRsoft.html#Nicolai>.